Received: 16 February 2021 | Revised: 28 September 2021 | Accepted: 9 October 2021

DOI: 10.1002/joc.7411

International Journal of Climatology RMetS

RESEARCH ARTICLE

The climatology of extreme wildfires in Portugal, 1980–2018: Contributions to forecasting and preparedness

Miguel Carmo[1,2] | **João Ferreira**[1] | **Manuel Mendes**[1] | **Álvaro Silva**[1] | **Pedro Silva**[1] | **Daniela Alves**[3] | **Luís Reis**[3] | **Ilda Novo**[1] | **Domingos Xavier Viegas**[3]

[1]Departamento de Meteorologia e Geofísica, Instituto Português do Mar e da Atmosfera (IPMA, IP), Lisbon, Portugal

[2]Institute of Contemporary History, NOVA FCSH, Lisbon, Portugal

[3]Forest Fires Research Centre, Association for the Development of Industrial Aerodynamics, Universidade de Coimbra, Coimbra, Portugal

Correspondence
Miguel Carmo, Divisão de Previsão Meteorológica, Vigilância e Observação da Terra, Departamento de Meteorologia e Geofísica, Instituto Português do Mar e da Atmosfera (IPMA, IP), Rua C do Aeroporto, Lisbon 1749-077, Portugal.
Email: miguelccarmo@gmail.com

Funding information
Fundação para a Ciência e a Tecnologia, Grant/Award Numbers: PCIF/GFC/0109/2017, UIDB/04209/2020, UIDP/04209/2020

Abstract

Available research has extensively examined the spatiotemporal patterns of fire-weather regime in Portugal, but a comprehensive climatology of extreme wildfires is still under development. This study calls for different strategies and scales of analysis aiming to describe the relationships between medium and low troposphere weather conditions and severe fire behaviour in mainland Portugal, between 1980 and 2018. In particular, critical fire-weather patterns and thresholds that can contribute to operational and forecasting know-how in short and medium time ranges are presented. We updated the general trends in the fire regime with a new, longer daily burned area series and developed a method that identifies Extreme Wildfire Periods (EWP) that form the basis for climate analysis. Synoptic analysis using Circulation Weather Types (CWT) showed that the northeasterly and easterly directional flows are significantly associated with EWP and produce the most severe fire-weather conditions. The four main CWT related to extreme fire are driven from anticyclones over the eastern Atlantic between the Azores and the British Isles. However, severe situations can also be regulated by CWT with marginal presence in both summer and EWP: low systems located to the west and northwest of Iberia carrying air masses from the south quadrant are related to catastrophic events. Regarding the antecedent climate, the results indicate that the coincident meteorological drought, whether weak or intense, is a necessary but not sufficient condition for the development of an EWP. An increasing relevance of water stress for shorter intervals preceding EWP, in the order of days and weeks, is apparent. Following these results, fine dead fuel moisture thresholds related to transitions in fire behaviour in Portuguese landscapes are computed using a promising predictive moisture content model. Finally, the different methods used are summoned for the detailed analysis of an EWP starting under unusual synoptic circulation.

KEYWORDS
coincident drought, dead fuel moisture thresholds, extreme wildfire periods, fire-prone weather types, western Iberia, wildfires climatology

1 | INTRODUCTION

Wildfires are socio-biophysical, complex phenomena (Minnich, 2001; Moreira *et al*., 2001; Fernandes *et al*., 2016a) with a long history on Earth (Pausas and Keeley, 2009; Pechony and Shindell, 2010). Their physical and ecological behaviour (e.g., rate of spread and land-use burning patterns) depends on multiple factors, such as ignitions sources, topography, land cover, fire suppression policies, forest management, and weather conditions, among others (Bessie and Johnson, 1995; Bowman *et al*., 2009; Carmo *et al*., 2011; Fernandes *et al*., 2012; Moreno *et al*., 2014; Turco *et al*., 2017).

In the last decades, fire regimes worldwide and especially in the Mediterranean climate regions, evolved to larger, high-intensity and uncontrolled wildfires resulting in large burned areas, destruction of ecosystems and infrastructures, soil erosion, and human life loss (Bastos *et al*., 2011; Moreira *et al*., 2011; Tedim *et al*., 2018; Madadgar *et al*., 2020; Tedim *et al*., 2020a). The case of Portugal is paradigmatic within Europe; it presents the highest density of both burned area and ignitions in recent decades. In 2003 and 2005, the annual burned areas broke national records and surpassed the total burned areas of Spain, France, Italy, and Greece combined (Silva *et al*., 2010; San-Miguel-Ayanz *et al*., 2013; San-Miguel-Ayanz *et al*., 2019). The last decade had a worst year (2017) with about 540,000 ha burned, 117 fatalities and fire fronts reaching rates of spread rarely recorded in literature (CTI, 2017; Tedim *et al*., 2018; Turco *et al*., 2019; Viegas *et al*., 2019).

This unexpectedly large magnitude remains, however, only partially understood. Weather is a well-documented critical factor in determining the timing and size of fires (Viegas and Viegas, 1994; Flannigan and Wotton, 2001; LePage *et al*., 2008) and extreme fire events rarely occur in the absence of severe weather conditions (Trigo *et al*., 2006; Moreira *et al*., 2011, 2020; Fernandes *et al*., 2016a; Pereira *et al*., 2020). Weather sciences are therefore decisive for the development of forecasting and preparedness approaches. In fact, research has extensively examined the spatiotemporal patterns of fire-weather regimes in Portugal (e.g., Pereira *et al*., 2005; Carvalho *et al*., 2008; Boer *et al*., 2017; Russo *et al*., 2017; Parente *et al*., 2018; Turco *et al*., 2019; Calheiros *et al*., 2020; Pereira *et al*., 2020), but a comprehensive climatology of extreme fire is still underdeveloped. In particular, changing frequencies of extreme weather and fire events demands an enhanced ability to predict when landscapes change from a nonflammable state to the highly flammable state necessary for catastrophic wildfires (Boer *et al*., 2017; Ruffault *et al*., 2018b).

After careful review of different strategies (see, e.g., the broad frameworks for studies on fires set by Flannigan and Wotton, 2001, and Pereira *et al*., 2020), the works of Crimmins (2006), Trigo and DaCâmara (2000), and Boer *et al*. (2017) became reference methods for this work, as will be seen below. Taken together, these studies show that extreme fire weather conditions should be thought of as part of a continuum of meteorological variability whose study imposes the combination of different scales of analysis, methods, and data. The overall objectives of this article are to (a) describe the relationships between upper and surface weather conditions and severe fire behaviour in mainland Portugal between 1980 and 2018, (b) address knowledge gaps in these interactions in the context of climate change, and (c) determine critical fire-weather patterns that improve operational know-how and forecasting ability in short and medium time ranges.

The following section presents the fire regime in Portugal and the Extreme Wildfire Periods (EWP) approach. Section 3 typifies large-scale circulation during the summer and EWP using an unsupervised synoptic climatology method. In Section 4, we analyse the contribution of the antecedent water balance in the development of severe fire. Then, in Section 5, a recent physical model of fine dead fuel moisture content is used to determine critical thresholds of fire behaviour transition. Section 6 provides a detailed analysis of an EWP that challenges the lessons learned from previous sections, followed by the concluding section.

2 | THE WILDFIRE REGIME IN PORTUGAL

2.1 | Fire data

Fire data were compiled from the Portuguese records of fire occurrence (ICNF, 2020). This is a raw database that has undergone important changes since 1980 in the reporting practices, presenting several inconsistencies (Carvalho and Lopes, 2001; Pereira *et al*., 2011). A systematic correction was made, which included the (a) elimination of fires with zero burned area and

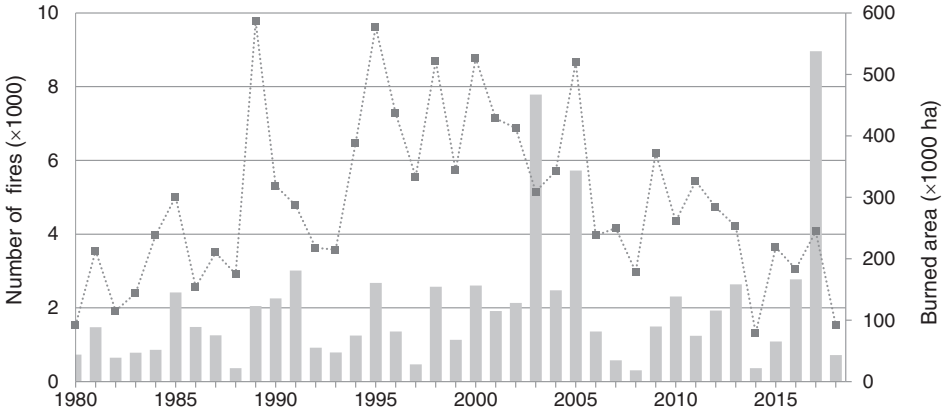

FIGURE 1 Annual burned area (bars) and number of fires (dotted line) between 1980 and 2018 (fires ≥ 1.0 ha)

duplicates with equal time, location and burned area, (b) adjustment of unrealistic durations of large wildfires based on information from media and reports, and (c) exclusion of fires with a burned area <1.0 ha, as the minimum logging area varied over time below this value.

We produced a database of individual fires with time coordinates, location (parish level) and land use (agriculture, forest, or scrub) (Table S1) and a nationwide daily time series of the burned area, resulting from the daily sum of the quotients between burned area and duration in days of each fire (Table S2). Although large fires do not have the same rate of spread from day to day and a decline is expected in the last few days until extinction, we consider the daily series a good approximation. The daily sum of area per day quotients highlights the most critical periods and clearly identifies the transition day to severe fire spread.

The final database presents 189,734 fires which burned 4.6 million ha between 1980 and 2018, respectively, 25.8 and 98.5% of the original totals. This database is available for future research as Supporting Information.

2.2 | Overall trends

The evolution of the annual burned area and fire frequency in the period 1980–2018 (Figure 1) does not show significant trends (Mann-Kendall test, $\rho \geq .05$). Yet, this should be approached cautiously, as discussed elsewhere (Pereira *et al.*, 2011; Silva *et al.*, 2019; Turco *et al.*, 2019), since this time series shows important interannual changes due to climate variability, as well as land use conversion perpetrated by fires themselves. The probability of burning depends on fuel age, increasing with time since the last fire. The modal and mean fire return intervals in Portugal were determined as 7 and 36 years, respectively, through a Weibull distribution in the period 1975–2005 (Oliveira *et al.*, 2011), which suggests that our 39-year study period may not be long enough to cover ongoing transitions. The record-breaking 2017 fire season may constitute an outlier or the beginning of a shift that will be clarified in future analysis (Silva *et al.*, 2019).

In a simple heuristic approach, the total burned area by decade (1980–1989: 724,371 ha, 1990–1999: 985,954 ha; 2000–2009: 1,582,607 ha; 2010–2019: 1,363,596) indicate a marked increase in the first three decades and a slight decrease in the last one. Moreover, the number of fires that burned more than 10,000 ha suggests a post-2000 change: 1 in the 1980–90s (burning about 10,000 ha), 11 in the 2000s (average burned area of 14,000 ha), and 16 in the 2010s (average of 25,000 ha). It is worth noting that the 3 years with the largest burned areas are 2017, 2003, and 2005.

The monthly distribution of burned area shows that the fire season is concentrated in July, August and September, which account for 81.3% of the total burned area in 1980–2018 (Figure S1). However, an increasing proportion of the annual burned area has been occurring outside the three summer months (Figure 2). This trend is confirmed by the gradual advance of the annual day on which the 10% of the annual burned area were exceeded (Figure 3). There was a significant move back from 44 days (on the 10% exceedance date) to 28 days (on the 20% date) in the beginning of the fire season (Mann-Kendall test, $\rho \leq 0.05$). The remaining exceedance dates, including the end of the fire season (the 80–100% exceedance dates) do not show significant trends. These results are in line with the expected lengthening of the fire season in Portugal during the 21st century (Moriondo *et al.*, 2006; Carvalho *et al.*, 2010), where a clearer sign was also identified on the fire season earliness compared to its prolongation into autumn. Our analysis shows, however, that the predicted lengthening (Moriondo *et al.*, 2006) has already been reached. Similar trends were obtained for recent decades in the U.S. south-west, based on weather data (Jain *et al.*, 2018) and fire activity (Westerling, 2016).

2.3 | The definition of extreme wildfire periods

Large fires have long been a subject of research (e.g., Brotak and Reifsnyder, 1977; Moreno, 1998). In

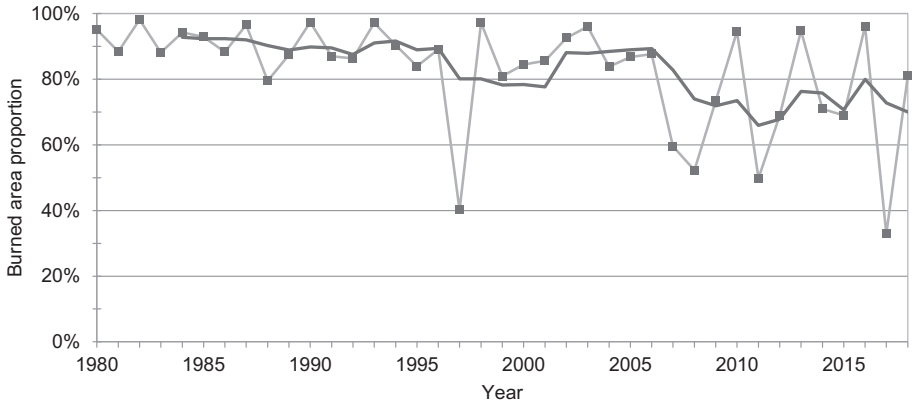

FIGURE 2 Annual evolution of the burned area proportion in the summer months (July, August and September) in relation to the annual total. The solid black line represents the 5-year moving averages

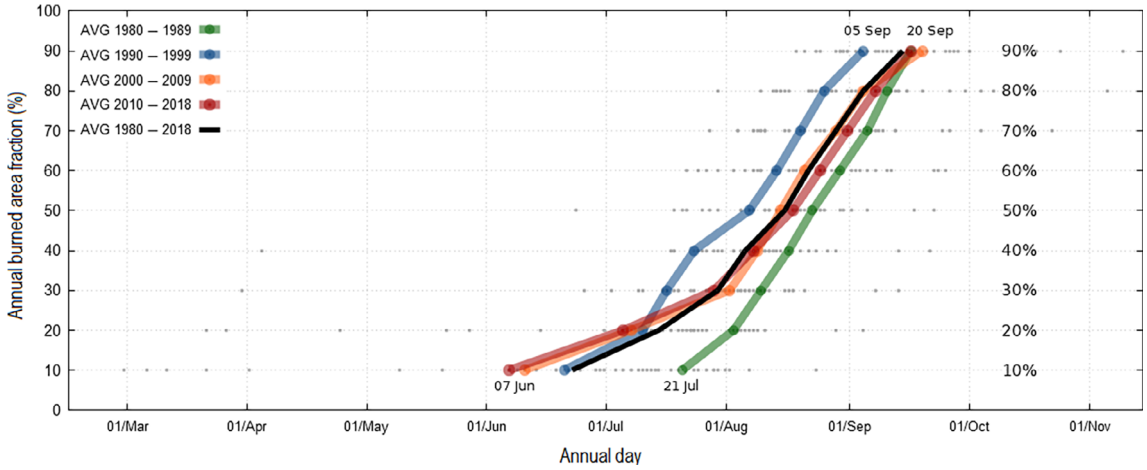

FIGURE 3 Exceeding dates for different fractions of the annual burned area (vertical axis). The grey dots represent the annual dates (39 dots in each fraction). The colour lines represent the decadal and all-period averages

southern Europe, different lower thresholds for defining large fires were used, ranging from 100 ha to 1,000 ha of burned area, usually based on the upper end of the fire size distributions (Lannom *et al.*, 2014; Fernandes *et al.*, 2016b). Recently, the limitations of classifications based solely on fire size have been underlined and new approaches to identify Extreme Wildfires Events are advocated. These are based on fire intensity (Bowman *et al.*, 2017), socioecological impacts (Moreira *et al.*, 2020), or multiple categories (Tedim *et al.*, 2018; Tedim *et al.*, 2020b). As a basis for our study, we developed a simple method that focuses however on *periods*, rather than events, of extreme fire behaviour. Our goal was to detect sequences of days with exceptional fire activity that would serve to identify extreme fire-weather relationships.

Extreme Wildfire Periods (hereafter, EWP) were obtained by a semi-automatic procedure, where the daily burned area time series was split in periods by mean-based segmentation (PELT method in 'changepoint' package, Killick and Eckley, 2014). After inspection of the obtained periods against the cumulative burned area curves, we (a) set a lower threshold of 3,000 ha·day^{-1} for the mean burned area of the EWP, and then (b) merged consecutive EWP into one, and (c) adjusted in few cases the length of the period to best cover the exceptional upward or downward variation in daily burned area. Figure S2 illustrates the determination of the EWP over a small interval of the time series.

We obtained 53 EWP, which total 392 critical days and a burned area equal to 52% of the total burned area in the 1980–2018 period. The EWP have variable duration, from 3 days (two cases) to 21 days (one case). The average duration is 7.4 days. With regard to monthly distribution, 3 EWP occurred in June (6%), 40 in July and August (75%), 7 in September (13%), and 3 in October (6%) (Appendix A1).

We find this method particularly useful to study small-sized regions, such as Portugal, where periods of severe fire-weather tend to affect much of the country (San-Miguel-Ayanz *et al.*, 2019). Moreover, it allows the precise identification of the first day when fire behaviour becomes extreme. In the last decades in Portugal, there were simultaneous extreme events that burned over 50,000 ha in short periods of 2–4 days (as seen in June and October 2017, Viegas *et al.*, 2017 and Viegas

et al., 2019), or extended periods with dozens of medium and large fires burning more than 350,000 ha (such as in August 2003, Trigo *et al.*, 2006).

3 | CRITICAL SYNOPTIC CIRCULATION

Linking large-scale circulation with surface weather and fire data is an effective way to build a synoptic climatology of extreme fire-weather (Crimmins, 2006). Several studies have examined synoptic patterns and circulation weather types (CWT) in relation to burned area, ignitions, and large fires (Brotak and Reifsnyder, 1977; Flannigan and Wotton, 2001; Skinner *et al.*, 2002; Rasilla *et al.*, 2010; Soriano *et al.*, 2013; Labosier *et al.*, 2015; Ruffault *et al.*, 2016; Trigo *et al.*, 2016), but few have employed these approaches to analyse the daily variability of severe fire conditions (Pereira *et al.*, 2005; Crimmins, 2006; DaCâmara and Trigo, 2018). Importantly, some papers have addressed the Iberian region which enables a discussion of results within different approaches.

We used a well-established, objective classification of atmospheric circulation, originally developed for the British Isles and later adapted to Portugal by Trigo and DaCâmara (2000). The calculation (described in detail in the cited work) is based on a set of indices of the direction and vorticity of the geostrophic flow that finally results in 26 CWT, either pure or hybrid. In our case, the daily synoptic classification from 1 January 1980 to 31 December 2018 was based on the mean sea-level pressure at 12 UTC provided by the ERA5 reanalysis (C3S, 2017), on a predefined 16-point grid (10°×5° longitude–latitude) covering a large North Atlantic area between 25°W–5°E and 30°–50°N.

3.1 | Critical weather types

The distribution of the 26 CWT during the summer shows a clear predominance of a small subset (Table 1) that agrees well with previous results (Trigo and DaCâmara, 2000). Regarding the EWP days, the NE (northeast) and E (east) directional types occurred in proportions that double (NE) and triple (E) their summer frequency and represent together about half of the critical days (48%). Chi-square tests between observed and expected day counts within each CWT confirmed that these two types had significantly ($p < .001$) more critical days than would be expected by chance alone. S (south) type is also significantly related to EWP, but was present in only 1.5% of EWP days (6/392 days). The A (anticyclonic) type was the only one that had significantly fewer days in the EWP than expected, still representing 6.4% of critical days.

The five most frequent types in the EWP represent together 75.3% of critical days, including the aforementioned 'fire prone' NE and E, plus the N (north) directional type and the two pure rotational types, A and C (cyclonic; see Figure S3). In addition, the frequency distribution for longer EWP shows an increasing predominance of the trio N, NE, and E from 63.7% (31 EWP ≥7 days) to 79.3% (8 EWP ≥11 days). Furthermore, day-to-day frequencies in the 4 days prior to the EWP shows a notable growth in the NE share, which reach a maximum on the first day of the EWP (55% for a summer average of 22%) and in the E share, which increases until the third day (15% for a summer average of 3%; Figure 4).

We will therefore focus on the NE, E, N, A, and C synoptic patterns and their mid- and low-tropospheric anomalies, considering the connections between Atlantic and European circulation and climatic anomalies over the Mediterranean region (Corte-Real *et al.*, 1995). Figure 5 presents multiple atmospheric fields and the respective composite anomalies at different levels for both the summer and EWP. Table 2 summarizes the overall average of field values over Portugal.

3.2 | The northeasterly and easterly fire-prone circulation

The NE an E summer circulations are characterized by high-pressure centres in the eastern Atlantic extending northeast and developing ridges over the Western Mediterranean. The Iberian thermal low is located in the southwestern Iberia, reinforcing the geostrophic flow over Portugal. In the case of NE, the Azores high extends to the Bay of Biscay and, during the EWP, the Moroccan thermal low extends northwards combining with the Iberian thermal low. The mean 500 hPa geopotential height (Z500) over Portugal increases 40 gpm between the summer and the EWP (Table 2). The E type shows a similar elongated SW–NE anticyclone localized further north between the British Isles and Iberia. The thermal low appears, in the summer and critical days, combined with the Moroccan thermal low affecting the south-central regions of Portugal.

In the NE summer, the composite daily mean temperatures at low-tropospheric levels show a persistent heating anomaly of 2–3°C while in the EWP they increase to the 5–6°C range. A similar, yet warmer pattern was obtained for the E type. In particular, the 2 m temperature during E critical days is the highest obtained in the five CWT (30.7°C), followed by the NE (30.2°C). Regarding the relative humidity, we found an expected negative anomaly in the NE summer flow, which intensifies during the EWP to

TABLE 1 The results of Chi-square tests between observed and expected day counts for each weather type. The bold *p*-values (<0.001) highlight the weather types with significantly more (or less) critical days than would be expected by chance alone

	A		**AN**		**ANE**		**AE**		**ASE**		**AS**		**ASW**	
Summer days	13.8%		7.4%		4.6%		0.5%		0.1%		0.1%		0.5%	
EWP days	6.4%		4.1%		4.6%		0.5%		0.5%		0.0%		0.0%	
	Obs.	Exp.	Obs.	Exp.	Obs.	Exp.	Obs.	Exp.	Obs.	Exp.	Obs.	Exp.	Obs.	Exp.
Critical days	25	54.1	16	29.2	18	18.2	2	1.8	2	0.3	0	0.2	0	2.0
Non-critical days	367	337.9	376	362.8	374	373.8	390	390.2	390	391.7	392	391.8	392	390.0
χ^2 *p*-value	**<.001**		.011		.960		.889		.004		.619		.159	
	AW		**ANW**		**C**		**CN**		**CNE**		**CE**		**CSE**	
Summer days	1.6%		3.8%		5.4%		1.4%		2.1%		1.2%		0.1%	
EWP days	0.0%		1.5%		8.2%		0.8%		1.8%		2.0%		0.3%	
	Obs.	Exp.	Obs.	Exp.	Obs.	Exp.	Obs.	Exp.	Obs.	Exp.	Obs.	Exp.	Obs.	Exp.
Critical days	0	6.3	6	15.1	32	21.2	3	5.6	7	8.2	8	4.7	1	0.5
Non-critical days	392	385.7	386	376.9	360	370.8	389	386.4	385	383.8	384	387.3	391	391.5
χ^2 *p*-value	.011		.017		.016		.268		.682		.125		.472	
	CS		**CSW**		**CW**		**CNW**		**N**		**NE**		**E**	
Summer days	0.2%		0.6%		0.5%		0.5%		17.8%		22.1%		3.0%	
EWP days	0.5%		0.0%		0.3%		0.5%		13.0%		38.0%		9.7%	
	Obs.	Exp.	Obs.	Exp.	Obs.	Exp.	Obs.	Exp.	Obs.	Exp.	Obs.	Exp.	Obs.	Exp.
Critical days	2	0.7	0	2.3	1	2.0	2	2.1	51	69.7	149	86.5	38	11.9
Non-critical days	390	391.3	392	389.7	391	390.0	390	389.9	341	322.3	243	305.5	354	380.1
χ^2 *p*-value	.143		.128		.486		.967		.014		**<.001**		**<.001**	

	SE		**S**		**SW**		**W**		**NW**	
Summer days	0.4%		0.3%		1.7%		3.7%		6.5%	
EWP days	1.0%		1.5%		0.8%		0.8%		3.3%	
	Obs.	Exp.	Obs.	Exp.	Obs.	Exp.	Obs.	Exp.	Obs.	Exp.
Critical days	4	1.4	6	1.3	3	6.7	3	14.5	13	25.5
Non-critical days	388	390.6	386	390.7	389	385.3	389	377.5	379	366.5
χ^2 *p*-value	.028		**<.001**		.152		.002		.011	

Note: The relative distribution of the 26 weather types in the EWP and summer days set the observed and expected critical day counts, respectively.

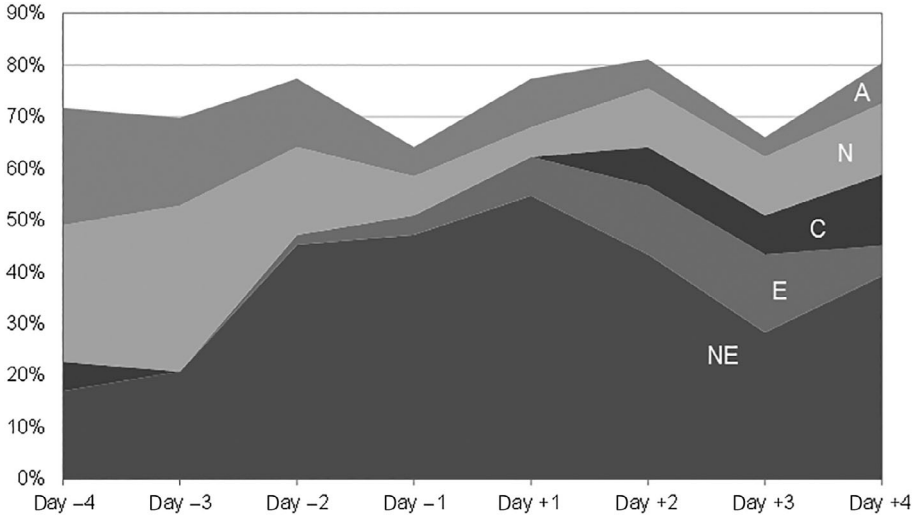

FIGURE 4 The daily distribution of the five most frequent weather types (NE, E, C, N, and A) in an 8-day window around the EWP onset (Day +1)

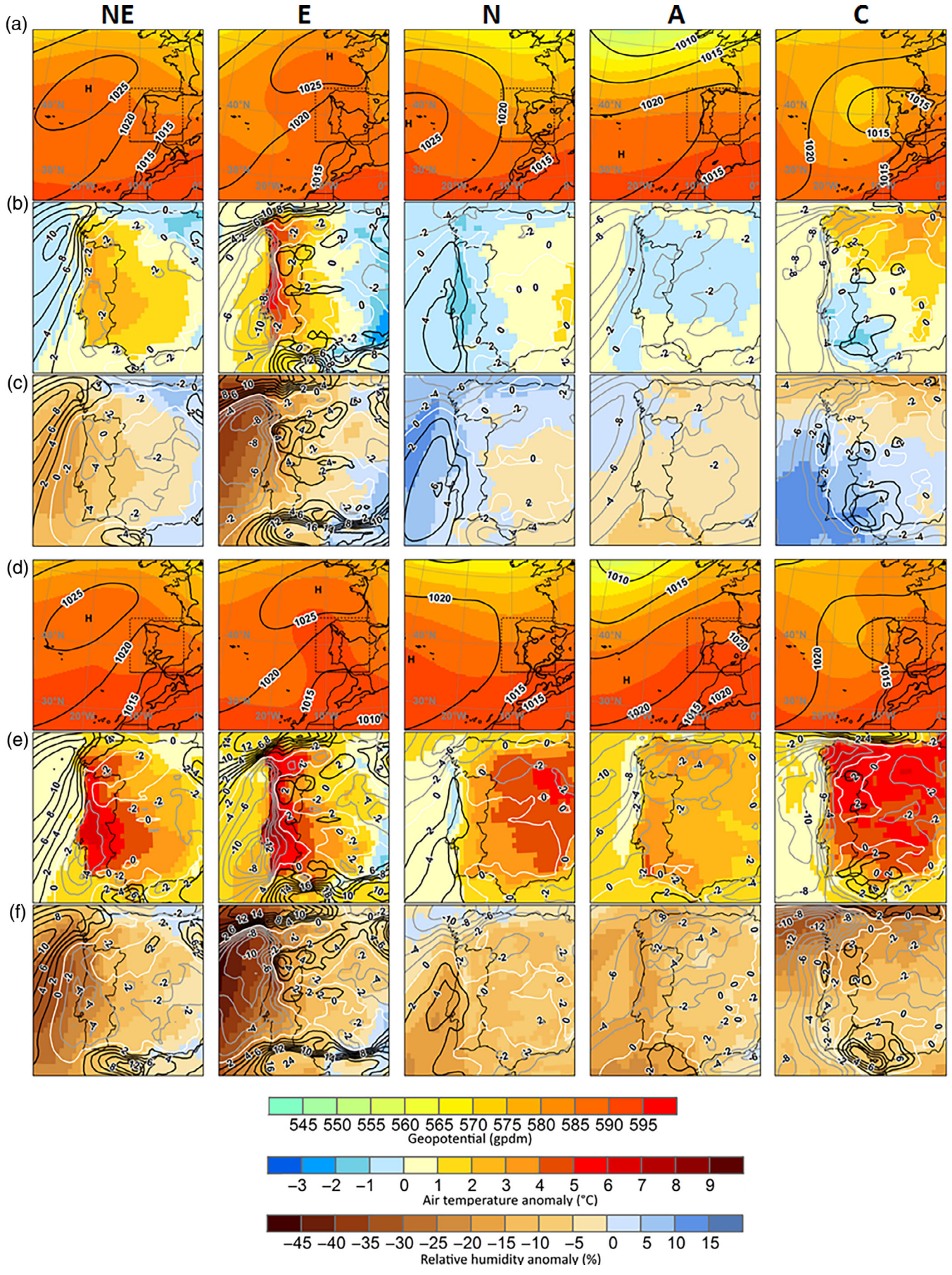

FIGURE 5 Legend on next page.

TABLE 2 The overall average values over Portugal and respective anomalies of multiple atmospheric fields, for each main CWT, during the summer (JJAS) and the EWP critical days

		NE		E		N		A		C	
	Period	**JJAS**	**EWP**	**JJAS**	**EWP**	**JJAS**	**EWP**	**JJAS**	**EWP**	**JJAS**	**EWP**
	Number of days	**1050**	**149**	**145**	**38**	**846**	**51**	**657**	**25**	**257**	**32**
Geopotential height (gpm)	500 hPa	5848	5888	5885	5906	5805	5858	5857	5903	5796	5856
	Anomaly	23.8	64.1	60.5	81.8	−19.6	33.6	32.6	78.6	−28.6	31.5
	Difference	40		21		53		46		60	
Temperature (°C)	850 hPa	15.6	19.1	16.9	19.0	11.9	18.0	12.8	17.3	13	19.7
	Anomaly	2.3	5.8	3.7	5.8	−0.7	5.4	−0.3	4.2	0.6	7.3
	925 hPa	21.8	24.6	23.2	24.6	18.6	22.5	19	22.2	20.1	24.5
	Anomaly	2.3	5.1	3.7	5.1	−0.9	3.0	−0.5	2.7	0.6	5.0
	2 m	27.3	30.2	29.3	30.7	24.1	27.5	25	28.2	25.3	29.5
	Anomaly	2.2	5.1	4.2	5.6	−1	2.4	−0.1	3.1	0.2	4.4
Relative humidity (%)	850 hPa	45.5	36.2	38.6	33.2	54.2	37.6	48.2	36.6	57.4	39.1
	Anomaly	−7.5	−16.8	−14.4	−19.8	1.2	−15.4	−4.7	−16.3	4.4	−13.9
	925 hPa	44.7	34.9	37.2	31.8	56.1	42.1	51.4	39.2	57.3	41.3
	Anomaly	−8.7	−18.5	−16.6	−22.0	2.8	−11.2	−2	−14.2	4	−12.0
Wind Intensity ($km \cdot h^{-1}$)	925 hPa	11.7	12.5	15.6	14.8	14.7	14.5	11.6	11.8	14.7	14.0
	Anomaly	−2.4	−1.6	1.5	0.7	0.5	0.3	−2.6	−2.4	0.6	−0.1
	10 m	8.9	9.1	10	9.9	11.3	11.2	9	8.7	10.3	9.8
	Anomaly	−1.5	−1.3	−0.2	−0.3	0.9	0.8	−1.4	−1.7	−0.1	−0.6

Note: Anomaly fields were computed with reference to the 1981–2010 summer period. Of note, 850 hPa geopotential height has the advantage of being representative of surface conditions without suffering from local effects. Information at 500 hPa is representative of the centre of gravity of the column and therefore can be a useful indicator of the entire tropospheric circulation.

−18.5% (925 hPa) and −16.8% (850 hPa). Again, E type shows the lowest values of relative humidity, in both tropospheric levels in summer and in EWP days.

The wind intensity fields of NE show null or slightly negative anomalies at 925 hPa and 10 m in both summer and critical days, although the latter shows some intensification. The E type show the highest mean wind intensity at the 925 hPa level (15.6 $km \cdot h^{-1}$ in summer and 14.8 $km \cdot h^{-1}$ in EWP), which translate into positive anomalies. Moreover, the E wind fields display well-demarcated regions in the North of the country with anomalies greater than 2, 4, and 6 $km \cdot h^{-1}$ and no apparent difference between the summer and EWP.

In summary, the northeasterly circulation worsens fire-weather summer conditions in temperature (warmer) and humidity (drier), but not in the wind intensity. On the critical days, temperature and relative humidity anomalies are further intensified. The Easterly circulation produces the most severe conditions among the five analysed CWT, both in summer and critical days. Importantly, type E presents the highest Z500 in summer and EWP days, as well as the smallest difference between the two (∼21 gpm). In fact, the difference between summer and EWP in the various parameters analysed is less pronounced in E, which seems to explain the largest difference between the frequencies in summer (3.0%) and in EWP (9.7%). Of the 145 days with Easterly flow in the 1980–2018 summers, 38 are included in the critical periods (26%), and 78 (54%) had a daily burned area greater than 500 ha.

FIGURE 5 Composite averages (period 1980–2018) and anomalies (reference period 1981–2010, June to September), for medium and low tropospheric fields, related to the weather types NE, E, N, A, and C (column one to five, respectively), during the June to September summer period (rows [a], [b], and [c]) and for EWP days in the same period (rows [d], [e] and [f]), namely: Mean sea level pressure (contour lines, 5 hPa interval) and Z500 (colour classes, 5 gpdm interval; rows a and d); anomalies of 10 m mean wind intensity (contour line, 2 $km \cdot hr^{-1}$ interval) and 2 m air temperature (colour classes, 1°C interval) (rows b and e); anomalies of 925 hPa wind intensity (contour line, 3 $km \cdot hr^{-1}$ interval) and 925 hPa relative humidity (colour classes, 5% interval; rows c and f). The dashed square encompassing Portugal in the circulation plots corresponds to the zoom area of the anomaly fields

3.3 | The northerly and anticyclonic flows

The N weather type represents a typical summer circulation over Portugal (the second most frequent after NE, with 18% of summer days), occurring less frequently in EWP. Type A is also common in summer (the third most) and as we have seen, it occurs significantly less in the EWP. Both CWT have higher frequencies in the days prior to the EWP, which then decrease and stabilize below their summer average (Figure 4).

The N circulation is characterized by a well-defined anticyclone displaced towards its summer position near the Azores archipelago, which produces northerly winds that are often reinforced by the development of a thermal low located over central Spain (Trigo and DaCâmara, 2000). The air masses transported over Portugal are mainly of maritime origin, which although modified by continental influence maintain high levels of humidity. The summer fields of relative humidity present, contrary to the NE and E types, a slightly positive anomaly that becomes negative during the EWP, yet showing wetter conditions compared to NE and E. N type summer temperatures are the lowest of the five CWT in the three tropospheric levels, which translates into negative anomalies. During EWP, conditions change substantially, which is comparable to the temperature transition seen in the Anticyclonic and Cyclonic types. Nonetheless, the 2 m temperature on critical days remains the lowest of the five types (27.5°C). On the contrary, the wind intensity at 925 hPa and 10 m show mean values among the highest, along with types E and C.

The Anticyclonic type shows an elongated Azores high extending in ridge towards Iberia. The resulting circulation at low levels is defined by the adjustment between the Iberian thermal low and the anticyclonic field. On critical days, a more developed ridge shows a slight intensification of the anticyclonic circulation over north-western Iberian Peninsula. In general, there are important differences between the summer and EWP climatological patterns, as also seen in type N. Type A conditions are also, on average, not particularly conducive to fires and the EWP days present harsher fire-weather conditions with temperature and relative humidity anomalies with an opposite sign. The wind intensity anomalies are negative, both in the summer and in the EWP.

3.4 | The challenging cyclonic type

Type C is more frequent in EWP compared to summer, but there is no clear significance ($p = .016$). After examining the day-to-day occurrence in each EWP, we found peculiar patterns: the cyclonic flow is absent in the 3 days preceding the EWP, only reappearing from the second EWP day at frequencies consistently above the summer average (compare Figure 4 and S3). Moreover, it regularly appears in sequences of days that close the critical periods; in 12 of the 53 EWP, which corresponds to 72% of the C critical days. This seems to suggest a contribution of cyclonic circulation in easing fire-weather conditions in the latter part of critical periods, which is, however, not firmly confirmed: the relative humidity composites show the less dry conditions among the main CWT (anomaly of −12.0%), but the temperature shows an important positive anomaly (+4.4°C).

In sharp contrast, cyclonic circulation is also associated with the early stages of some exceptionally severe EWP. These very unusual situations marked the recent history of fires in Portugal: on the 2–3 of August 2003 (Trigo *et al*., 2006); 18–20 June 2017 (Moreira *et al*., 2017; Sánchez-Benítez *et al*., 2018; Turco *et al*., 2019), and on 15 October 2017 (Novo *et al*., 2018; Calheiros *et al*., 2020). During these days, cyclonic circulation carried hot and dry air from the south and southeast originating in North Africa, usually with intensified wind fields.

Cyclonic large-scale circulation presents a low-pressure centre over the Portuguese west coast. In the mid-troposphere, there is a well-defined inverse omega shape that leads to a closed cyclonic circulation in the southern part. Type C has, at the type E antipodes, the largest gradient in the Z500 between summer and EWP. The relationship between summer depressions and extreme fire requires further research with particular attention to the development of upper tropospheric lows temporally cut-off from the main western stream, phenomena well studied on the Iberian Peninsula (Nieto *et al*., 2005; Nieto *et al*., 2007).

3.5 | Final overview

Overall, the results indicate that the meteorological conditions during the EWP are an intensification of the typical summer climate in Portugal. During the critical days, all five critical CWT show higher Z500 and low-troposphere temperatures accompanied by lower relative humidity. The wind intensity does not show a clear pattern between summer and EWP. In short, the synoptic configurations related to extreme fire behaviour in Portugal correspond in the vast majority to dry and hot flows generated by anticyclonic regimes located to the west-north quadrant of Iberia; that is, by the northerly, northeasterly, easterly, and anticyclonic types. Nevertheless, severe situations can be also regulated by depressions located to the west and northwest of Iberia, carrying air masses from the south quadrant, revealed by the greater frequency of types C, S, and SE.

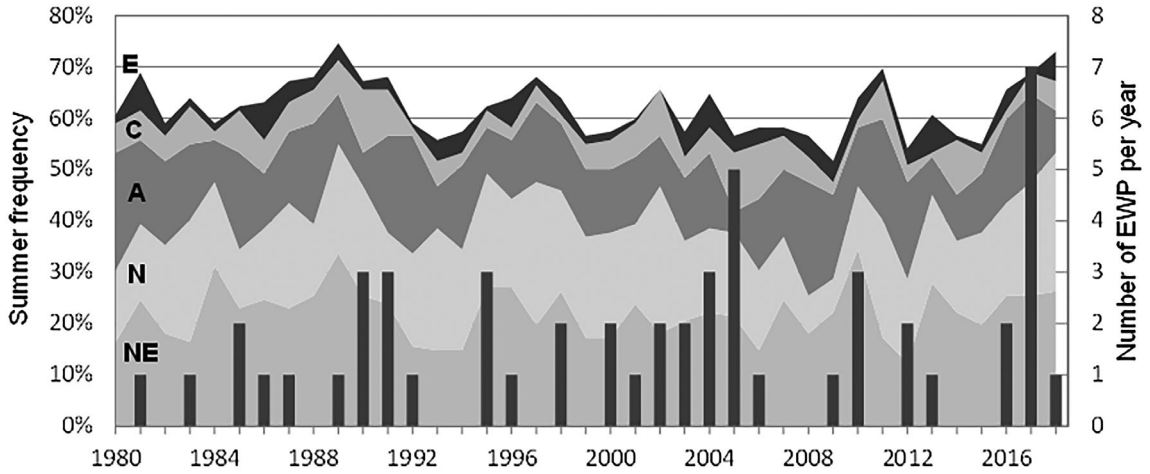

FIGURE 6 Annual distribution of the five critical CWTs summer frequencies (NE, N, A, C, E) between 1980 and 2018. The solid bars and the right y-axis represent the number of EWP per year

The primacy of the northeasterly and easterly flows in the western Iberia severe fire-weather was identified in previous studies (Soriano *et al*., 2013; Amraoui *et al*., 2015; Trigo *et al*., 2016; DaCâmara and Trigo, 2018), although using different methods and smaller time frames. Pereira *et al*. (2005) describes the prevalence of southeast advection from northern Africa in the development of large fires that does not stand out in our results: the sum of types SE, ASE, CSE does not reach 2% of EWP days and type C, which include days with southeast flow, accounts 8.2%.

Despite general similarities, the climatology of the examined CWT suggests distinct interactions with fire near the surface and therefore differentiated fire-weather regimes: wind-driven, heat-driven and drought-driven fires (following Ruffault *et al*., 2016 and Ruffault *et al*., 2018b; Duane and Brotons, 2018). Easterly circulation produced the warmest, driest and windiest conditions, thus combining the wind-, heat-, and drought-driven regimes that gives it the label of most fire-prone. Northeasterly flow is similarly hot and dry, slightly less than the E, but not windy (negative anomaly), so it appears to configure a fire regime forced by heat and dryness. In contrast, Northerly circulation had the highest wind intensity and is one of the 'coldest' and 'wettest', so it clearly forms a wind-driven regime. The anticyclonic flow was comparatively not very hot and windy, but very dry (although less than E and NE types), which suggests a regime mainly controlled by the continuous drying of fuels. Finally, type C shows intermediate conditions of temperature and wind, and comparatively high relative humidity, not being easily included in any of the three regimes.

We finally hypothesized that the changes in extreme fire behaviour from 1980 (see Section 2), could stem from an increasing presence of NE and E types in summer. However, the annual evolution of the five critical CWT summer frequencies does not reveal any synoptic trend; there is an apparent constancy in the distribution of the main CWT over the 39-year period (Figure 6). The findings of section 3 can help understanding the synoptic climatology of extreme fires and provide elements to assess in advance the fire danger in Portugal based on circulation models. Lastly, both Pereira *et al*. (2005) and Trigo *et al*. (2016) showed that despite the good response of burned area variability to the short-term synoptic forcing, the models fit improve when the antecedent climate is also included. This scale of analysis is the focus of the next section.

4 | SEASONAL DROUGHT CONTRIBUTION

For several decades, fire-weather research has sought to clarify the influence of the seasonal and interannual water balance in the fire season, having identified conflicting effects of lagged precipitation in above normal fire activity (Viegas and Viegas, 1994; Koutsias *et al*., 2013; Pereira *et al*., 2013; Pilliod *et al*., 2017; Tramblay *et al*., 2020). The links between drought and fire have undergone relevant changes in recent centuries (Swetnam and Betancourt, 1998; Hessl *et al*., 2004) and are receiving renewed attention in the face of a changing climate (Dimitrakopoulos *et al*., 2011; Boer *et al*., 2016; Gouveia *et al*., 2016; Ruffault *et al*., 2018b). In particular, these studies show that although a strong relation between drought and fires exist, drought alone is not sufficient to predict burned area values, in part because the development of the water balance throughout the year(s) can produce opposite effects, either limiting or promoting fuel growth and controlling the moisture content of fuels at variable time lags.

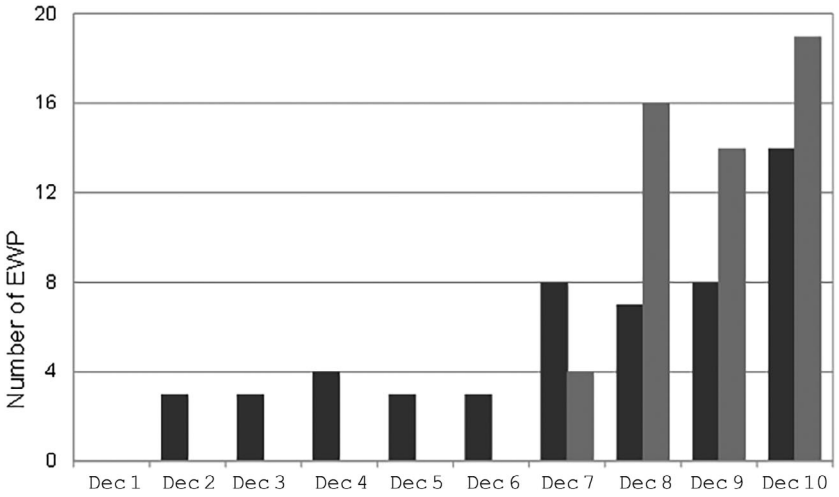

FIGURE 7 The decile distribution of absolute (grey bars) and relative (black bars) percentiles of drought code values on the first day of the 53 extreme wildfire periods

Recent comprehensive studies indicate that the spring–summer drought conditions leading to the fire season ('coincident drought') play a dominant role for fires in Portugal (Pereira *et al*., 2005; Russo *et al*., 2017; Parente *et al*., 2019), Mediterranean Europe (Gudmundsson *et al*., 2014; Turco *et al*., 2017; Tramblay *et al*., 2020) and United States (Riley *et al*., 2013; Littell *et al*., 2016) when compared to longer-term climatic conditions. In short, as the time window for the drought indices lengthens, correlations with fire weaken (Riley *et al*., 2013; Higuera *et al*., 2015; Littell *et al*., 2016; Russo *et al*., 2017). However, studies on drought contribution to extreme fire development are still emerging and major uncertainties remain (Riley *et al*., 2013; Littell *et al*., 2016; Ruffault *et al*., 2018b; Madadgar *et al*., 2020). In the following sections, we examined the intensity and time signature of seasonal drought at the EWP onset.

4.1 | The water deficit when extreme fire starts

We used well-established metrics that track seasonal changes (drying or wetting) of fuels, namely, the Drought Code (DC), the slowest drying component of the FWI System (Van Wagner, 1974), and the Palmer Drought Severity Index (PDSI) (Palmer, 1965) calibrated for Portugal (Pires, 2003). The DC and PDSI are cumulative indices of long memory, providing drought ratings at the beginning of the EWP that are blind to the way the water balance developed in the preceding months or years. Both indices are widely used in fire-drought studies (e.g., Riley *et al*., 2013; Littell *et al*., 2016; Ruffault *et al*., 2018b) and are included in IPMA's national fire and drought monitoring systems.

The absolute percentage rank of the DC values (1980–2018 period) in the first day of the 53 EWP shows that the vast majority (49/53) started with DC values above the 70th percentile. The minimum DC required to 'trigger' an EWP is low (DC = 171, 61th percentile) and the distribution in the seventh (16 EWP), eighth (14), and ninth (19) deciles shows no trend. Furthermore, the *relative* percentage rank of onset DC values within the series of 39 same days (e.g., 1 September 1980, ..., 1 September 2018) shows that EWP can start on days with particularly low DC values for what is expected in that date (Figure 7).

The PDSI analysis showed that most EWP (43/53) occurred in months with index below −0.5 (that is, 'weak', 'moderate', 'severe', or 'extreme' drought), of which 30 under weak or moderate drought and only 13 under severe or extreme drought. Finally, the scatter plots of the PDSI and absolute percentile of DC against the mean daily burned area of each EWP show no significant trend, although there appears to be a weak positive correlation after 2000, absent in the previous period (Figure 8).

These results indicate, as also suggested by Parente *et al*. (2019), that a coincident drought, whether of low, moderate or high intensity is a necessary but not sufficient condition for extreme fire behaviour (see complete data in Appendix A1).

4.2 | Long versus short-term drought: In search of time signatures

We first analysed the response of the accumulated precipitation (based on gridded estimates of daily totals from ERA5 reanalysis) preceding the EWP onset in successively shorter periods of time: 64, 32, 16, and 8 days. Each period reduction in half was accompanied by a systematic reduction in the average accumulated precipitation around 1/3 (Table 3). In fact, only the shortest interval (8 days) shows

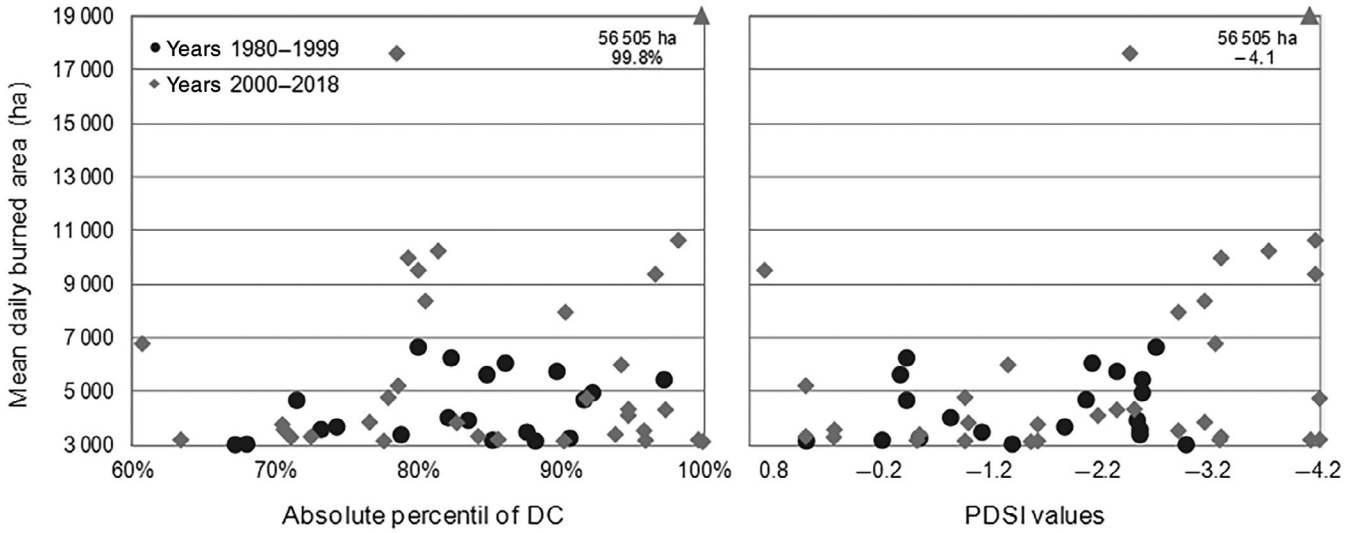

FIGURE 8 Scatter plots of absolute percentile of DC (left graph) and PDSI (right graph) against the mean daily burned area of the EWP. The black balls represent the 1980–1999 period and the grey diamonds the following period (2000–2018); the triangular sign with the associated coordinates represents a single point outside the displayed Y-scale

	64 Days	32 Days	16 Days	8 Days
EWP average (mm)	33.9	10.7	4.2	1.4
SD	18.6	8.1	5.5	1.8
Fraction of the previous interval		32%	39%	34%

TABLE 3 The average accumulated precipitation at the beginning of the 53 EWP for different preceding intervals (64, 32, 16, and 8 days). The ratio between the averages of successive intervals are shown

null precipitation in all EWP (average = 1.4 mm, *SD* = 1.8). This suggests an increasing relevance of the water deficit for smaller periods close to the beginning of EWP. In addition, the accumulated precipitation anomalies of the preceding 64-days interval (with reference to the same days average in 1980–2018), show that 12 EWP had a null or positive deviation (≥0 mm) averaging an anomaly of +16 mm. Therefore, 23% of the EWP, corresponding to 27% of the critical days, occurred after 2 months of normal-to-wet conditions.

The rising relevance of shorter-term water balance in the development of severe fire can also be observed by the comparative distribution of the absolute percentiles of DC and Fine Fuel Moisture Code (FFMC, the fastest drying component of the FWI System). As mentioned, all EWP started with DC values above the 61th percentile and are evenly distributed in the seventh, eighth, and ninth deciles, while the FFMC values are all above the 79th percentile with the majority (45/53) above the 90th percentile. This comparison agrees well with Nash and Johnson (1996), where the increasing probability of lightning-caused fire occurrence with decreasing fuel moisture is evident with the FFMC and shows no trend with the DC. Based on these results, the next section focuses on the response of fine fuel moisture content.

5 | FINE FUEL MOISTURE THRESHOLDS

The moisture level of landscape fine fuels is a critical element of fire behaviour (Simard and Main, 1982; Viegas *et al*., 1992; Flannigan *et al*., 2013; Viegas *et al*., 2013; Nolan *et al*., 2016a) and one of the most used and oldest indicators in predicting weather fire risk (Curry and Fons, 1940; Van Wagner, 1974; Van Wagner, 1990; Wotton, 2008; Rossa and Fernandes, 2017). Recent work has found that low fine fuel moisture content may determine when large fires can occur, advocating close relationships between moisture thresholds and fire behaviour transitions (Fernandes *et al*., 2008; Dennison and Moritz, 2009; Nolan *et al*., 2016b; Boer *et al*., 2017). However, although subject to long-standing research, a widely accepted model for estimating the moisture content of fine fuels is still missing (Sharples and McRae, 2011; Matthews, 2014; Nolan *et al*., 2016a; Nolan *et al*., 2016b) and large differences are found in the ability of drought indices and empirical models to predict actual fine fuel moisture content (DeDios *et al*., 2015; Ruffault *et al*., 2018a). The following analysis focuses exclusively on dead fuel, leaving aside the dynamics of live fuel with fire.

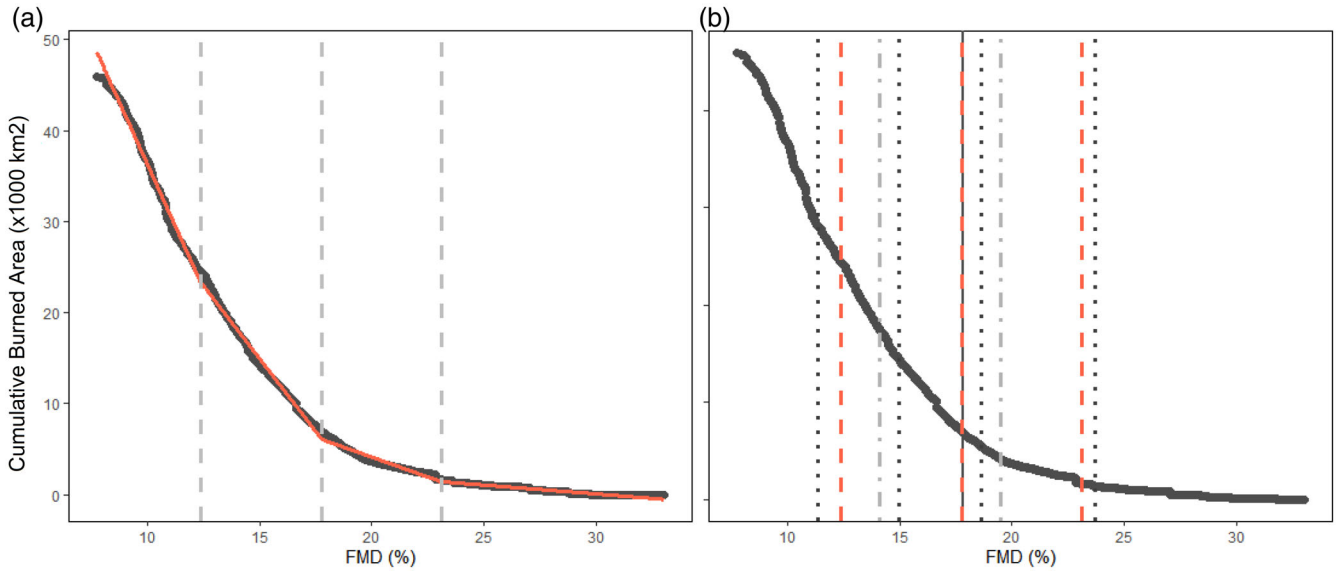

FIGURE 9 Relationship between cumulative burned area in Portugal (1980–2018) and predicted fine dead fuel moisture content (FMD) with adjusted linear regressions for different numbers of breakpoints. The graph on the left (a) shows multiple linear regressions fitted to either side of three breakpoints, as in previous analyses (Boer *et al.*, 2017). The graph on the right (b) shows the relative position of the breakpoints obtained when considering only one (black solid line), two (grey dash-dotted line), three (red dashed line), or four (black dotted line) possible thresholds (see Table 4 for breakpoint values)

TABLE 4 Breakpoint values obtained in the different runs (with 1, 2, 3, and 4 breakpoints) with the multiple R^2 and *SE* obtained

Breakpoints in FM_D (%)					Multiple R^2	*SE*
1-BP			17.8		.9906	0.009
2-BP		14.1	19.5		.9975	≤0.02
3-BP	12.4		17.8	23.1	.9988	≤0.02
4-BP	11.3	14.9	18.6	23.7	.9996	≤0.02

We computed moisture thresholds related to transitions in fire severity in Portugal using a promising semi-mechanistic model for estimate the moisture content of fine dead fuel (DeDios *et al.*, 2015; Nolan *et al.*, 2016a; Nolan *et al.*, 2016b; Boer *et al.*, 2017). The FM_D model is based on the exponential decline of moisture content with increasing vapour pressure deficit and depends on well-established meteorological parameters, making it particularly suitable for forecasting. It is supported by a physical basis, unlike most rating systems (see Van Wagner, 1974 regarding the FWI), and was successfully compared with other models commonly used in fire danger ratings (DeDios *et al.*, 2015; Nolan *et al.*, 2016a). FM_D is a function of vapour deficit (D), as detailed in Nolan *et al.* (2016a):

$$FM_D = FM_0 + FM_1 \cdot \exp(-mD), \quad (1)$$

where $FM_0 = 6.79$ is minimum FM_D, $FM_1 = 27.43$ ($FM_0 + FM_1$ is the maximum FM_D when D is null), and $m = 1.05$ is the rate of change in FM_D with D. D is the daily difference between mean saturation vapour pressure (e_s) and actual vapour pressure (e_a) (Monteith and Unsworth, 2013):

$$D = e_s - e_a, \quad (2)$$

$$e_s = 0.6108 \cdot \exp\left(17.27 \cdot \frac{T_{air}}{T_{air} + 237.15}\right), \quad (3)$$

$$e_a = 0.6108 \cdot \exp\left(17.27 \cdot \frac{T_d}{T_d + 237.15}\right), \quad (4)$$

where T_{air} and T_d are daily mean air and dew-point temperatures, respectively, obtained from gridded estimates of ERA5 reanalysis and averaged over mainland Portugal.

5.1 | Critical thresholds of fire severity

The cumulative daily burned area in Portugal was plotted as a function of FM_D along the 1980–2018 period, following the procedures of Dennison and Moritz (2009) and using our daily burned area time series instead of allocating the total area of the fire to the day the fire started (as in Dennison and Moritz, 2009; Nolan *et al.*, 2016a; Boer *et al.*, 2017). Segmented regression was used to adjust linear regressions on both sides of the curve breakpoints (Muggeo, 2008).

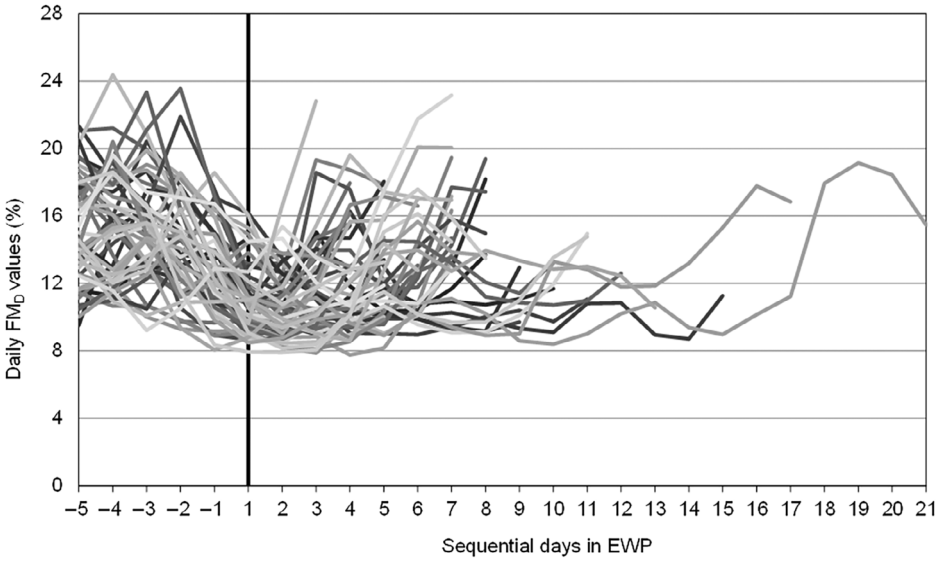

FIGURE 10 Daily variation of the FMD in each of the 53 EWP, differentiated on a grey scale, from the fifth day before the start of each period until the last day. The bold vertical line indicates the first day of the EWP

We first forced one breakpoint only and then increased the number to four to assess the persistence of the obtained transitions. The results show that the 1-breakpoint transition persists in all others runs (2-, 3- and 4-breakpoints) in the range 17.8–19.5% of predicted fine dead fuel moisture content (Figure 9b). Moreover, the transitions determined in each run reappeared in at least another run (Table 4).

The 3-breakpoints analysis (Figure 9a) agrees well with previous results for Portugal (Boer *et al*., 2017), where the thresholds 12, 18, and 26% were obtained from a reduced period (2001–2015). However, our upper threshold was 23.1%, differing by almost 3%. The days with $FM_D > 23.1\%$ add up to less than 3.5% of the total area burned in 1980–2018, presenting an average daily burned area of 21 ha. Moreover, the 23.1% threshold is consistently below reported moisture content edging sustained combustion and fire extinction (27–39% in Fernandes *et al*., 2008, 25–35% in Boer *et al*., 2017, 24.2% in Leonard, 2009), which suggests that under real, historical conditions a reduced danger level was persistently reached for FM_D above 23%, where fire spread is likely weakened and more susceptible to fire suppression. Experimental burns on four shrub fuel types in natural conditions in Portugal showed that spread rate exponentially decline with dead fuel moisture content, reaching a low plateau from the 20–25% range (Fernandes, 2001).

The lower moisture threshold obtained in the 3-breakpoints analysis (12.4%) is close to large-fire thresholds found in Yellowstone National Park, United States (13%) (Renkin and Despain, 1992), across U.S. ecoregions (11.4–14.5; Nagy *et al*., 2018), in distinct eucalypt ecosystems in southeastern Australia (12.4–15.1%; Nolan *et al*., 2016b), and in boreal and subalpine forests in Alberta and Saskatchewan, Canada (14%; Nash and Johnson, 1996).

Finally, a recent pertinent note on potential biases resulting from the cumulative burnt area method (see Pimont *et al*., 2019) was considered carefully. As shown in Figure S4, our long FM_D series has a quite uniform distribution in the range where breakpoints were detected (∼12–26%) so the risk of bias was set aside (Pimont F, 2021, pers. comm.).

5.2 | Characteristic FM_D initiating EWP

The daily variation of the FM_D in each EWP, from the fifth day before the start of the period until the last day (Figure 10), reveals a prominent valley of very low moisture content between the first and the third day of the EWP. For longer periods, this minimum peak can last up to 1 or 2 weeks. The overall mean of FM_D in the first 3 days is 11.2% ($SD = 2.4$), which is below the lower moisture threshold obtained with 3-breakpoints and the aforementioned literature thresholds, and very close to the lower threshold obtained with 4-breakpoints (11.3%). Consequently, the use of four thresholds, which includes an ultimate transition for very extreme fire around 11%, can be relevant in Portugal. It is worth noting that days with $FM_D < 8\%$ are extremely rare (only 4 in the 39-year period) and are all included in the first 3 days of the EWP.

The mean FM_D of the 5 days leading up to the EWP shows decreasing values from the fifth day before (average of 15.2%) until the EWP's eve (12.8%). Lastly, all EWP came to an end at FM_D values below 23.2%, averaging 15% in the last day, which reinforce the upper obtained thresholds of 17–18% and 23–24% as transitions to reduced fire danger. Our analysis confirmed that FM_D is a good determinant of the area burned by wildfires in

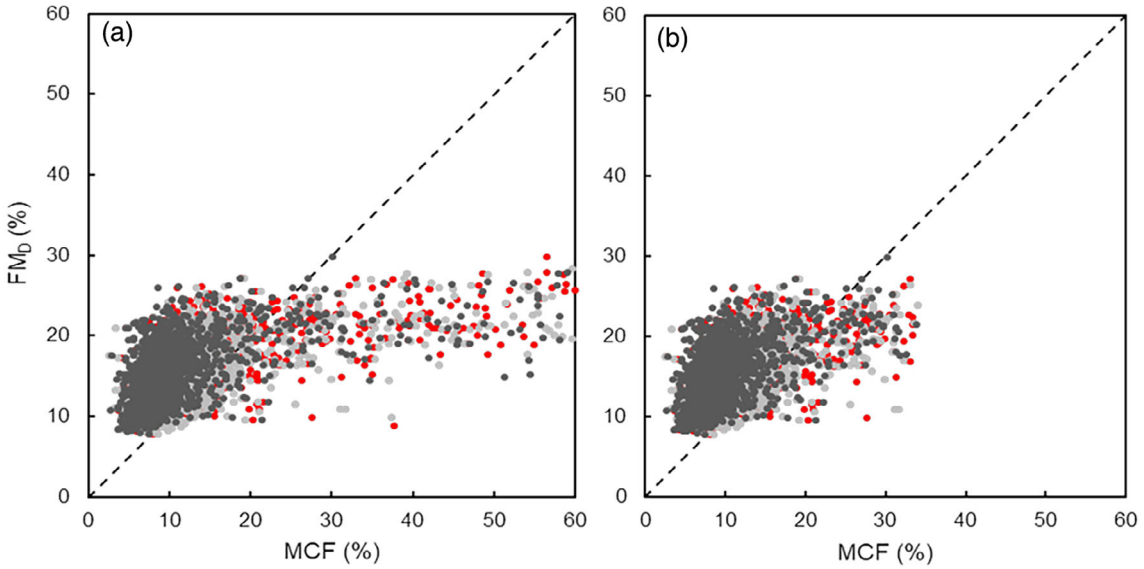

FIGURE 11 Scatter plots of daily FMD and MCF of dead pine needles (light grey balls), dead eucalyptus leaves (dark grey balls), and the average of both (red balls). The graph on the left shows the series without restrictions in the period 1996–2018 (not all points are displayed as the MCF has values above 60%). The graph on the right shows the series restricted to the summer period (June to September) and limited upwards by 34.2%

Portugal, even when a nationwide approach is used, and can provide a solid tool for predicting critical flammability transitions. The large coincidence of the minimum FM_D values and the onset of EWP (first 3 days) revealed by Figure 10 shows the suitability of both methodologies.

5.3 | The FM_D model against long-term measures in Central Portugal

The FM_D model was compared with a long series of fine fuel moisture measurements made in central Portugal, where pine and eucalyptus planted forests are the main contributors to the soil blanket of dead fuels. The moisture content of these fuels has been monitored in a south oriented slope in Lousã, Coimbra since 1987 by the Forest Fire Research Centre (CEIF-ADAI, University of Coimbra) (Viegas *et al*., 1992; MCFire, 2018). Although the data are localized (considered a good proxy for the central region, Viegas and Viegas, 1994), comparison with the national FM_D series is useful as a first approach to the model performance in Portugal.

The sample collection is done daily at 12 p.m. from 15th May to 15th October and two times a week in the rest of the year. For each species, five samples of initial mass *Mi* are placed in an oven at 105°C for 24 hr and weighed again, *Mf*. The daily moisture content on a dry basis of each sample,

$$\mathrm{MCF} = \frac{Mi - Mf}{Mf}, \tag{5}$$

is averaged for each fuel type. We considered dead pine needles (PN) and eucalyptus leaves (EL) collected from the soil surface, and a third series with the daily average of PN and EL values (APE), producing a database of 2081 days with MCF and FM_D values in the 1996–2018 period (data prior to 1996 were dismissed for reasons of consistency).

Figure 11a shows a good development of the point cloud around the 1:1 axis for MCF values below about 30%, followed by a persistent deviation afterwards. The resulting large positive differences between MCF and FM_D are due, on one hand, to concomitant dry air conditions (low FM_D) and accumulated rain water in the soil that hinders the drying of the dead fuels (high MCF). On the other hand, the FM_D model was designed to perform in the very low moisture range and has an asymptotic upper limit of 34.2% (see Equation 1). For a better comparison, the series range was restricted to the summer period and by the upper limit of FM_D (Figure 11b). The FM_D shows a positive bias until the MCF values reach around 20%. After this value, the point cloud is largely displayed below the 1:1 axis. The overall FM_D bias in relation to the three MCF series is in the range 3.2–5.5%, while the MAE varies between 4.4 and 6.2% (Table 5). The PN series show the smallest differences to the FM_D predictions. Future model developments should include

regional analysis and explore calibration with data for Portugal.

6 | A CRITICAL PERIOD IN DETAIL: 22–29 SEPTEMBER 1983

Calling on the various scales and methods addressed before, we analysed an EWP that took place under infrequent synoptic circulation conditions in the summer. On 22 September 1983, a period of severe fire began that lasted 8 days and had a burned area of 27,971 ha, 96% of which in the central Portuguese region (daily evolution in Table 6). The meteorological drought during September, given by the PDSI, extended to the south-central regions with moderate intensity. The DC at the beginning of the EWP is high (361, 88th absolute percentile), but comparatively low for the end of the summer (34th relative percentile).

The week preceding the EWP had predominant anticyclonic circulation (CWT A) governed by a typical summer high pressure located south of the Azores. On 22–24 September (hereafter, Phase I), the blocking system (e.g., Alvarez-Castro *et al*., 2018) evolves by the intensification and displacement northeastward of the anticyclone to the British Isles. In accordance, the western low of the omega block located to the northwest of Iberia moves southward and approaches Portugal, establishing a southwest flow (Day 22) and an intensified south flow over the next 2 days. Phase I produced a decrease in Z500 to values similar to the summer average. The southwest and then south flow transported maritime air masses with rising temperatures and relative humidity over Portugal and, more substantially, higher wind intensity. FM_D values dropped to less than 14.9%, the second severity threshold from 4-breakpoints analysis, and the mean FWI in central Portugal increased to the upper fire danger class (FWI > 38.2, Palheiro *et al*., 2006). This phase had the highest burned area and number of active fires in the EWP.

TABLE 5 Summary of the error estimates between the restricted series of FMD predictions and MCF measurements (Figure 11b) for dead pine needles (PN), dead eucalyptus leaves (EL), and the daily arithmetic average of both (APE)

	PN	EL	APE
Number of points	1437	1464	1335
Bias	3.2	5.5	4.2
MAE	4.4	6.2	5.1
r^2	.25	.25	.26

Note: Bias is the mean bias error, MAE is the mean absolute error, and r^2 is the linear correlation coefficient.

TABLE 6 Daily summaries for the EWP of 22–29 September 1983

			Phase I			Phase II			Phase III	
	Summer average	21/09	22/09	23/09	24/09	25/09	26/09	27/09	28/09	29/09
CWT		A	SW	S	S	A	A	A	SW	W
Burned area (ha)		706	4,567	4,974	4,837	1,975	3,200	3,511	2,668	2,239
Active fires		49	75	101	93	76	62	60	56	27
Z500 (gpm)	5818	5884	5855	5816	5887	5967	5928	5863	5791	5729
Anomaly		66	37	−2	69	149	110	45	−27	−89
Surface temperature (2 m) (°C)	25.5	26.8	29.6	28.1	29.0	28.3	30.4	29.9	27.4	22.4
Anomaly		1.3	4.1	2.6	3.5	2.8	4.9	4.4	1.9	−3.1
Relative humidity (925 hPa) (%)	55.1	35.9	36.5	48.8	50.0	50.4	30.3	28.6	40.2	61.4
Anomaly		−19.2	−18.6	−6.3	−5.1	−4.7	−24.8	−26.5	−14.9	6.3
Wind intensity (925 hPa) ($km \cdot h^{-1}$)	20.4	4.6	21.1	30.3	30.7	9.9	9.7	9.8	8.7	14.0
Anomaly		−15.8	0.7	9.9	10.3	−10.5	−10.7	−10.6	−11.7	−6.4
Dew point temperature (2 m) (°C)	12.8	11.4	12.9	13.0	14.1	14.4	12.3	10.8	13.0	13.0
Anomaly		−1.4	0.1	0.2	1.3	1.6	−0.5	−2.0	0.2	0.2
Total precipitation (mm)		0	0	0	0	0	0	0	0.2	0
FWI		25.6	35.9	44.4	45.4	28.7	35.9	35.8	31.3	22.1
FM_D		15.0	13.1	13.7	14.0	14.0	11.6	11.8	14.3	19.4

Note: The mean values and anomalies were determined for the central region of Portugal based on ERA5 reanalysis data. FM_D values represent the entire territory.

On 25–27 September (Phase II), the blocking system moves to the northwest, re-establishing the anticyclonic circulation in Portugal. Low small nuclei are formed during the day in the south-central regions of Iberia. The Z500 reaches its maximum with +149 gpm anomaly (Day 25). The subsidence movement of the air produced by an intense anticyclone gradually decreased the relative humidity and a new slight rise in temperature occurred. The atmospheric stability characteristic of these situations produced a great reduction in the wind intensity. The FWI dropped to the Very High class ($24.6 < FWI < 38.2$), but the FM_D continued to fall due to a greater difference between air and dew point temperatures (Phase II average of 12.5%). The intensity of the fire fronts shows some reduction, with daily burned areas around 3,000 ha.

On 28–29 September (Phase III), the blocking system moves back to the east, now at higher latitudes, and its western low approaches the northwest of Iberia again, re-establishing a southwest flow on the 28th that runs west on the 29th, the last day of the EWP. The change in circulation brought an important decrease in Z500 and on the last day negative and positive anomalies of temperature and relative humidity, respectively. As a consequence, FM_D rose to 19.4%, on the way to the low danger level, the FWI dropped to 22.1 (High level), and the EWP ended. The day after (30 September), the national burned area is 41 ha and there are seven active fires.

The EWP broke out within a fire-weather regime controlled by the wind and temperature, where the rise in relative humidity did not prevent maximum fire risk and burned areas (wind-driven). During Phase II, fire is driven by low winds and increasing vapour pressure deficit (drought-driven). The examination of this EWP daily summaries show that extreme fire can be strongly regulated by synoptic patterns with marginal presence in both the summer and the subset of critical periods. This case reinforces the relevance of cyclogenesis located to the west and northwest of the Portuguese coast, driving intensified flows from the south quadrant over mainland, which was also identified at the beginning of some remarkable EWP (see Section 3.4): while in the present EWP the air masses were in the beginning predominantly maritime, coming from southwest, in the EWP triggered under type C flow, the advection of dry and windy southeast air masses from North Africa gave them greater catastrophic dimension.

7 | CONCLUSIONS

In this study, we aimed to develop a comprehensive climatology of extreme wildfires in Portugal, whose new magnitude and social emergency has been accompanied by few, recent climatological and meteorological studies. This is indeed a rapidly developing field - facing new dynamics that result from concomitant key changes in the landscape fuels and climate to which this article contributes.

The EWP approach developed allowed isolating the critical fire periods from the long series of records (1980–2018) in view of the exploratory concatenation of well-established climatological scales and approaches. This simple method identifies periods of extreme fire behaviour, rather than events, and provided a good basis for daily climate analysis. Without the EWP, it would not be possible to test complementarities/continuities between methods/scales. In the previous section, we explored the integration of different methods in a concrete historical example, while gaining critical perspective on the object of study: situations with very low frequency within the critical periods can be the most serious and challenging from a scientific and management point of view.

We found that although the annual burned area in Portugal does not show significant trends in the 1980–2018 period, the occurrence of very large fires is a differentiating characteristic of the post-2000 period. The analysis of the fire season revealed its widening, with a clear anticipated start.

It has been shown that synoptic patterns related to extreme fire mainly derive from anticyclones centred in the Azores region generating directional flows over Portugal from the north, northeast and east, and anticyclonic flow. These large circulation similarities produce, however, different surface conditions and different fire-weather climatologies. The easterly and northeasterly types produce the most severe conditions, as also identified in previous studies. However, results also showed that extreme fire can be regulated by unusual synoptic patterns in the summer. Cyclogenesis located to the west and northwest of Iberia, forcing flows from the southern quadrant, are related to the most extreme fire events in the studied period. Finally, we did not detect any climatic trend in the distribution of synoptic patterns in the summer from 1980 onward.

Regarding the antecedent climate, the coincident drought, not necessarily intense, appears as a necessary condition for extreme fire. Importantly, water stress is increasingly relevant in the imminence of the EWP. In this sense, the fine dead fuel moisture content thresholds based on the 4-breakpoints calculus are a solid, necessary tool for predicting critical transitions of flammability in Portuguese landscapes in short time ranges.

ACKNOWLEDGEMENTS

Work was developed under the project FIRESTORM, Weather and Behaviour of Fire Storms funded by FCT/MCTES (PCIF/GFC/0109/2017). The authors thank

to Vanda Pires who calculated the PDSI index for Portuguese climatological stations and to the IPMA colleagues from FIRESTORM, Nuno Moreira, Paulo Pinto, João Rio, Jorge Neto, and Maria José Monteiro. Authors are also grateful to colleagues at ADAI and the MCFire project (PCIF/MPG/0108/2017) for providing MCF data, and to ICNF for providing rural fire records. M.C. is now based at the Institute of Contemporary History (NOVA FCSH, Lisbon), which is funded by FCT/MCTES (UIDB/04209/2020 and UIDP/04209/2020). We would like to extend a special thanks to IPMA for the weather data and other facilities made available for this work. Finally, we dedicate this study to the memory of professor and climatologist João M. Corte-Real.

AUTHOR CONTRIBUTIONS

Miguel Costa Carmo: Conceptualization; data curation; formal analysis; methodology; writing – original draft; writing – review and editing. **João Ferreira:** Data curation; formal analysis; software. **Manuel Mendes:** Data curation; formal analysis; software. **Álvaro Pimpão Silva:** Conceptualization; data curation; formal analysis; software. **Pedro Silva:** Data curation; formal analysis; software. **Daniela Sofia Alves:** Data curation; formal analysis; writing – original draft. **Luís Duarte Reis:** Data curation; formal analysis; writing – original draft. **Ilda Novo:** Conceptualization; data curation; methodology; project administration; writing – original draft. **Domingos Xavier Viegas:** Conceptualization; formal analysis; funding acquisition; methodology; project administration.

ORCID

Miguel Carmo https://orcid.org/0000-0002-4784-5997

REFERENCES

Alvarez-Castro, C., Faranda, D. and Yiou, P. (2018) Atmospheric dynamics leading to west European summer hot temperatures since 1851. *Complexity*, 2018, 2494509.

Amraoui, M., Pereira, M.G., DaCamara, C.C. and Calado, T.J. (2015) Atmospheric conditions associated with extreme fire activity in the Western Mediterranean region. *Science of the Total Environment*, 524, 32–39.

Bastos, A., Gouveia, C.M., da Câmara, C.C. and Trigo, R.M. (2011) Modelling post-fire vegetation recovery in Portugal. *Biogeosciences*, 8, 3593–3607.

Bessie, W.C. and Johnson, E.A. (1995) The relative importance of fuels and weather on fire behavior in subalpine forests. *Ecology*, 76(3), 747–762.

Boer, M.M., Bowman, D.M., Murphy, B.P., Cary, G.J., Cochrane, M.A., Fensham, R.J., Krawchuk, M.A., Price, O.F., Resco De Dios, V., Williams, R.J. and Bradstock, R.A. (2016) Future changes in climatic water balance determine potential for transformational shifts in Australian fire regimes. *Environmental Research Letters*, 11(6), 065002.

Boer, M.M., Nolan, R.H., De Dios, V.R., Clarke, H., Price, O.F. and Bradstock, R.A. (2017) Changing weather extremes call for early warning of potential for catastrophic fire. *Earth's Future*, 5(12), 1196–1202.

Bowman, D.M., Balch, J.K., Artaxo, P., Bond, W.J., Carlson, J.M., Cochrane, M.A., D'Antonio, C.M., DeFries, R.S., Doyle, J.C., Harrison, S.P., Johnston, F.H., Keeley, J.E., Krawchuk, M.A., Kull, C.A., Marston, J.B., Moritz, M.A., Prentice, I.C., Roos, C.I., Scott, A.C., Swetnam, T.W., van der Werf, G.R. and Pyne, S.J. (2009) Fire in the Earth system. *Science*, 324, 481–484.

Bowman, D.M., Williamson, G.J., Abatzoglou, J.T., Kolden, C.A., Cochrane, M.A. and Smith, A.M. (2017) Human exposure and sensitivity to globally extreme wildfire events. *Nature Ecology & Evolution*, 1(3), 1–6.

Brotak, E.A. and Reifsnyder, W.E. (1977) An investigation of the synoptic situations associated with major wildland fires. *Journal of Applied Meteorology*, 16(9), 867–870.

Calheiros, T., Nunes, J.P. and Pereira, M.G. (2020) Recent evolution of spatial and temporal patterns of burned areas and fire weather risk in the Iberian Peninsula. *Agricultural and Forest Meteorology*, 287, 107923.

Carmo, M., Moreira, F., Casimiro, P. and Vaz, P. (2011) Land use and topography influences on wildfire occurrence in northern Portugal. *Landscape and Urban Planning*, 100(1–2), 169–176.

Carvalho, A., Flannigan, M.D., Logan, K.A., Gowman, L.M., Miranda, A.I. and Borrego, C. (2010) The impact of spatial resolution on area burned and fire occurrence projections in Portugal under climate change. *Climatic Change*, 98(1–2), 177–197.

Carvalho, A., Flannigan, M.D., Logan, K.A., Miranda, A.I. and Borrego, C. (2008) Fire activity in Portugal and its relationship to weather and the Canadian Fire Weather Index System. *International Journal of Wildland Fire*, 17(3), 328–338.

Carvalho, J.B. and Lopes, J.P. (2001) *Classificação de Incêndios Florestais: Manual do utilizador*. Lisboa: Direcção-Geral das Florestas, p. 34 p. Available at:. http://www2.icnf.pt/portal/florestas/dfci/inc/manuais/classif-incend-flor.

Copernicus Climate Change Service (C3S). 2017. ERA5: Fifth generation of ECMWF atmospheric reanalyses of the global climate. C3S Climate Data Store (CDS). Available at: https://cds.climate.copernicus.eu/cdsapp#!/home [Accessed 2020].

Corte-Real, J., Zhang, X. and Wang, X. (1995) Large-scale circulation regimes and surface climatic anomalies over the Mediterranean. *International Journal of Climatology*, 15(10), 1135–1150.

Crimmins, M.A. (2006) Synoptic climatology of extreme fire-weather conditions across the Southwest United States. *International Journal of Climatology*, 26(8), 1001–1016.

CTI. (2017). Análise e Apuramento de Factos Relativos Aos Incêndios Que Ocorreram em Pedrogão Grande, Castanheira de Pêra, Ansião, Alvaiázere, Figueiró Dos Vinhos, Arganil, Góis, Penela, Pampilhosa da Serra, Oleiros e Sertã, entre 17 e 24 de Junho de 2017. Comissão Técnica Independente (CTI). Lisboa: Assembleia da República.

Curry, J.R. and Fons, W.L. (1940) Forest-fire behavior studies. *Mechanical Engineering*, 62, 219–225.

DaCâmara, C.C. and Trigo, R.M. (2018) Circulation weather types and their influence on the fire regime in Portugal. In: Viegas, D.X. (Ed.) *Advances in Forest Fire Research 2018, Ch. 3.*

Coimbra: Imprensa da Universidade de Coimbra, pp. 372–380. https://doi.org/10.14195/978-989-26-16-506_40.

DeDios, V.R., Fellows, A.W., Nolan, R.H., Boer, M.M., Bradstock, R.A., Domingo, F. and Goulden, M.L. (2015) A semi-mechanistic model for predicting the moisture content of fine litter. *Agricultural and Forest Meteorology*, 203, 64–73.

Dennison, P.E. and Moritz, M.A. (2009) Critical live fuel moisture in chaparral ecosystems: a threshold for fire activity and its relationship to antecedent precipitation. *International Journal of Wildland Fire*, 18(8), 1021–1027.

Dimitrakopoulos, A.P., Vlahou, M., Anagnostopoulou, C.G. and Mitsopoulos, I.D. (2011) Impact of drought on wildland fires in Greece: implications of climatic change? *Climatic Change*, 109(3–4), 331–347.

Duane, A. and Brotons, L. (2018) Synoptic weather conditions and changing fire regimes in a Mediterranean environment. *Agricultural and Forest Meteorology*, 253, 190–202.

Fernandes, P.M. (2001) Fire spread prediction in shrub fuels in Portugal. *Forest Ecology and Management*, 144(1–3), 67–74.

Fernandes, P.M., Botelho, H., Rego, F. and Loureiro, C. (2008) Using fuel and weather variables to predict the sustainability of surface fire spread in maritime pine stands. *Canadian Journal of Forest Research*, 38(2), 190–201.

Fernandes, P.M., Loureiro, C., Magalhães, M., Ferreira, P. and Fernandes, M. (2012) Fuel age, weather and burn probability in Portugal. *International Journal of Wildland Fire*, 21(4), 380–384.

Fernandes, P.M., Monteiro-Henriques, T., Guiomar, N., Loureiro, C. and Barros, A.M. (2016a) Bottom-up variables govern large-fire size in Portugal. *Ecosystems*, 19(8), 1362–1375.

Fernandes, P.M., Pacheco, A.P., Almeida, R. and Claro, J. (2016b) The role of fire-suppression force in limiting the spread of extremely large forest fires in Portugal. *European Journal of Forest Research*, 135(2), 253–262.

Flannigan, M., Cantin, A.S., De Groot, W.J., Wotton, M., Newbery, A. and Gowman, L.M. (2013) Global wildland fire season severity in the 21st century. *Forest Ecology and Management*, 294, 54–61.

Flannigan, M.D. and Wotton, B.M. (2001) Climate, weather, and area burned. In: Johnson, E.A. and Miyanishi, K. (Eds.) *Forest Fires: Behavior and Ecological Effects, Ch. 10*. San Diego, CA: Academic Press, pp. 351–373.

Gouveia, C.M., Bistinas, I., Liberato, M.L., Bastos, A., Koutsias, N. and Trigo, R. (2016) The outstanding synergy between drought, heatwaves and fuel on the 2007 southern Greece exceptional fire season. *Agricultural and Forest Meteorology*, 218, 135–145.

Gudmundsson, L., Rego, F.C., Rocha, M. and Seneviratne, S.I. (2014) Predicting above normal wildfire activity in southern Europe as a function of meteorological drought. *Environmental Research Letters*, 9(8), 084008.

Hessl, A.E., McKenzie, D. and Schellhaas, R. (2004) Drought and Pacific decadal oscillation linked to fire occurrence in the inland Pacific northwest. *Ecological Applications*, 14(2), 425–442.

Higuera, P.E., Abatzoglou, J.T., Littell, J.S. and Morgan, P. (2015) The changing strength and nature of fire-climate relationships in the northern Rocky Mountains, USA, 1902–2008. *PLoS One*, 10(6), e0127563.

ICNF. (2020). IncêndiosRurais – Estatísticas. Instituto da Conservação da Natureza e das Florestas (ICNF). Fire occurrence database. Available at: http://www2.icnf.pt/portal/florestas/dfci/inc/estat-sgif. [Accessed 26th March 2020].

Jain, P., Wang, X. and Flannigan, M.D. (2018) Trend analysis of fire season length and extreme fire weather in North America between 1979 and 2015. *International Journal of Wildland Fire*, 26(12), 1009–1020.

Killick, R. and Eckley, I. (2014) Changepoint: an R package for change point analysis. *Journal of Statistical Software*, 58(3), 1–19.

Koutsias, N., Xanthopoulos, G., Founda, D., Xystrakis, F., Nioti, F., Pleniou, M., Mallinis, G. and Arianoutsou, M. (2013) On the relationships between forest fires and weather conditions in Greece from long-term national observations (1894–2010). *International Journal of Wildland Fire*, 22(4), 493–507.

Labosier, C.F., Frauenfeld, O.W., Quiring, S.M. and Lafon, C.W. (2015) Weather type classification of wildfire ignitions in the Central Gulf Coast, United States. *International Journal of Climatology*, 35(9), 2620–2634.

Lannom, K.O., Tinkham, W.T., Smith, A.M.S., Abatzoglou, J., Newingham, B.A., Hall, T.E., Morgan, P., Strand, E.K., Paveglio, T.B., Anderson, J.W. and Sparks, A.M. (2014) Defining extreme wildland fires using geospatial and ancillary metrics. *International Journal of Wildland Fire*, 23, 322–337.

Leonard, S. (2009) Predicting sustained fire spread in Tasmanian native grasslands. *Environmental Management*, 44(3), 430–440.

LePage, Y., Pereira, J.M.C., Trigo, R., Câmara, C., Oom, D. and Mota, B. (2008) Global fire activity patterns (1996-2006) and climatic influence: an analysis using the World Fire Atlas. *Atmospheric Chemistry and Physics*, 8(7), 1911–1924.

Littell, J.S., Peterson, D.L., Riley, K.L., Liu, Y. and Luce, C.H. (2016) A review of the relationships between drought and forest fire in the United States. *Global Change Biology*, 22(7), 2353–2369.

Madadgar, S., Sadegh, M., Chiang, F., Ragno, E. and AghaKouchak, A. (2020) Quantifying increased fire risk in California in response to different levels of warming and drying. *Stochastic Environmental Research and Risk Assessment*, 34(12), 2023–2031.

Matthews, S. (2014) Dead fuel moisture research: 1991–2012. *International Journal of Wildland Fire*, 23(1), 78–92.

MCFire Project. (2018). Measuring the moisture content of forest fuels and assessing their behaviour within the new climate realities. Available at: https://adai.pt/mcfire/en/home-en/ [Accessed 11th December 2020]

Minnich, R.A. (2001) An integrated model of two fire regimes. *Conservation Biology*, 15(6), 1549–1553.

Monteith, J. and Unsworth, M. (2013) *Principles of Environmental Physics: Plants, Animals, and the Atmosphere*, 4th edition. Amsterdam: Elsevier Academic Press.

Moreira, F., Ascoli, D., Safford, H., Adams, M., Moreno, J.M., Pereira, J.C., Catry, F., Armesto, J., Bond, W.J., Gonzalez, M., Curt, T., Koutsias, N., McCaw, L., Price, O., Pausas, J., Rigolot, E., Stephens, S., Tavsanoglu, C., Vallejo, R., Van Wilgen, B., Xanthopoulos, G. and Fernandes, P. (2020) Wildfire management in Mediterranean-type regions: paradigm change needed. *Environmental Research Letters*, 15(1), 11001.

Moreira, F., Rego, F.C. and Ferreira, P.G. (2001) Temporal (1958–1995) pattern of change in a cultural landscape of northwestern Portugal: implications for fire occurrence.Landscape. *Ecology*, 16(6), 557–567.

Moreira, F., Viedma, D., Arianoutsou, M., Curt, T., Koutsias, N., Mouillot, F., Vaz, P., Barbati, A., Corona, P., Rigolot, E., Xanthopoulos, G. and Bilgili, E. (2011) Landscape–wildfire interactions in southern Europe: implications for landscape management. *Journal of Environmental Management*, 92, 2389–2402.

Moreira, N., Barbosa, S., Correia, S., Cota, T., Novo, I., Pinto, P., Rio, J. and Silva, A. (2017) *Condições meteorológicas associadas ao incêndio de Pedrógão Grande de 17 junho 2017*. Lisboa: Instituto Português do Mar e da Atmosfera. https://doi.org/10.13140/RG.2.2.11284.55686.

Moreno, J.M. (Ed.). (1998) *Large Forest Fires*. Leyden: Backhuys Publishers, p. 245.

Moreno, M.V., Conedera, M., Chuvieco, E. and Pezzatti, G.B. (2014) Fire regime changes and major driving forces in Spain from 1968 to 2010. *Environmental Science & Policy*, 37, 11–22.

Moriondo, M., Good, P., Durao, R., Bindi, M., Giannakopoulos, C. and Corte-Real, J. (2006) Potential impact of climate change on fire risk in the Mediterranean area. *Climate Research*, 31(1), 85–95.

Muggeo, V.M. (2008) Segmented: an R package to fit regression models with broken-line relationships. *R News*, 8(1), 20–25.

Nagy, R., Fusco, E., Bradley, B., Abatzoglou, J.T. and Balch, J. (2018) Human-related ignitions increase the number of large wildfires across US ecoregions. *Fire*, 1(1), 4.

Nash, C.H. and Johnson, E.A. (1996) Synoptic climatology of lightning-caused forest fires in subalpine and boreal forests. *Canadian Journal of Forest Research*, 26(10), 1859–1874.

Nieto, R., Gimeno, L., Anel, J.A., LaTorre, L., Gallego, D., Barriopedro, D., Gallego, M., Gordillo, A., Redaño, A. and Delgado, G. (2007) Analysis of the precipitation and cloudiness associated with COLs occurrence in the Iberian Peninsula. *Meteorology and Atmospheric Physics*, 96(1–2), 103–119.

Nieto, R., Gimeno, L., LaTorre, L., Ribera, P., Gallego, D., García-Herrera, R., García, J.A., Nuñez, M., Redaño, A. and Lorente, J. (2005) Climatological features of cutoff low systems in the Northern Hemisphere. *Journal of Climate*, 18(16), 3085–3103.

Nolan, R.H., Boer, M.M., De Dios, V.R., Caccamo, G. and Bradstock, R.A. (2016b) Large-scale, dynamic transformations in fuel moisture drive wildfire activity across southeastern Australia. *Geophysical Research Letters*, 43(9), 4229–4238.

Nolan, R.H., De Dios, V.R., Boer, M.M., Caccamo, G., Goulden, M. L. and Bradstock, R.A. (2016a) Predicting dead fine fuel moisture at regional scales using vapour pressure deficit from MODIS and gridded weather data. *Remote Sensing of Environment*, 174, 100–108.

Novo, I., Pinto, P., Rio, J. and Gouveia, C. (2018) Fires in Portugal on 15th October 2017: a catastrophic evolution. In: Viegas, D.X. (Ed.) *Advances in Forest Fire Research 2018, Ch. 1*. Coimbra: Imprensa da Universidade de Coimbra, pp. 57–70. https://doi.org/10.14195/978-989-26-16-506_5.

Oliveira, S.L., Pereira, J.M.C. and Carreiras, J.M. (2011) Fire frequency analysis in Portugal (1975–2005) using Landsat-based burned area maps. *International Journal of Wildland Fire*, 21(1), 48–60.

Palheiro, P.M., Fernandes, P. and Cruz, M.G. (2006) A fire behaviour-based fire danger classification for maritime pine stands: comparison of two approaches. *Forest Ecology and Management*, 234S, S54.

Palmer, W.C. (1965). Meteorological drought. Res. Pap. 45. US Department of Commerce, Weather Bureau. Washington, DC. p. 65.

Parente, J., Amraoui, M., Menezes, I. and Pereira, M.G. (2019) Drought in Portugal: current regime, comparison of indices and impacts on extreme wildfires. *Science of the Total Environment*, 685, 150–173.

Parente, J., Pereira, M.G., Amraoui, M. and Fischer, E.M. (2018) Heat waves in Portugal: current regime, changes in future climate and impacts on extreme wildfires. *Science of the Total Environment*, 631, 534–549.

Pausas, J.G. and Keeley, J.E. (2009) A burning story: the role of fire in the history of life. *Bioscience*, 59(7), 593–601.

Pechony, O. and Shindell, D.T. (2010) Driving forces of global wildfires over the past millennium and the forthcoming century. *Proceedings of the National Academy of Sciences*, 107(45), 19167–19170.

Pereira, M.G., Calado, T.J., da Câmara, C.C. and Calheiros, T. (2013) Effects of regional climate change on rural fires in Portugal. *Climate Research*, 57(3), 187–200.

Pereira, M.G., Malamud, B.D., Trigo, R.M. and Alves, P.I. (2011) The history and characteristics of the 1980-2005 Portuguese rural fire database. *Natural Hazards & Earth System Sciences*, 11, 3343–3358.

Pereira, M.G., Parente, J., Amraoui, M., Oliveira, A. and Fernandes, P.M. (2020) The role of weather and climate conditions on extreme wildfires. In: *Extreme Wildfire Events and Disasters, Root Causes and New Management Strategies*. Amsterdam: Elsevier, pp. 55–72.

Pereira, M.G., Trigo, R.M., da Câmara, C.C., Pereira, J.M. and Leite, S.M. (2005) Synoptic patterns associated with large summer forest fires in Portugal. *Agricultural and Forest Meteorology*, 129(1–2), 11–25.

Pilliod, D.S., Welty, J.L. and Arkle, R.S. (2017) Refining the cheatgrass–fire cycle in the Great Basin: precipitation timing and fine fuel composition predict wildfire trends. *Ecology and Evolution*, 7(19), 8126–8151.

Pimont, F., Ruffault, J., Martin-StPaul, N.K. and Dupuy, J.L. (2019) A cautionary note regarding the use of cumulative burnt areas for the determination of fire danger index breakpoints. *International Journal of Wildland Fire*, 28(3), 254–258.

Pires, V. (2003). *Frequência e intensidade de fenómenos meteorológicos extremos associados a precipitação*. MSc Dissert. Faculty of Sciences of the University of Lisbon. p. 98.

Rasilla, D.F., García-Codron, J.C., Carracedo, V. and Diego, C. (2010) Circulation patterns, wildfire risk and wildfire occurrence at continental Spain. *Physics and Chemistry of the Earth*, 35(9–12), 553–560.

Renkin, R.A. and Despain, D.G. (1992) Fuel moisture, forest type, and lightning-caused fire in Yellowstone National Park. *Canadian Journal of Forest Research*, 22(1), 37–45.

Riley, K.L., Abatzoglou, J.T., Grenfell, I.C., Klene, A.E. and Heinsch, F.A. (2013) The relationship of large fire occurrence with drought and fire danger indices in the western USA, 1984–2008: the role of temporal scale. *International Journal of Wildland Fire*, 22(7), 894–909.

Rossa, C.G. and Fernandes, P.M. (2017) On the effect of live fuel moisture content on fire-spread rate. *Forest Systems*, 26(3), 12.

Ruffault, J., Curt, T., StPaul, N.M., Moron, V. and Trigo, R.M. (2018b) Extreme wildfire events are linked to global-change-

type droughts in the northern Mediterranean. *Natural Hazards and Earth System Sciences*, 18, 847–856.

Ruffault, J., Moron, V., Trigo, R.M. and Curt, T. (2016) Daily synoptic conditions associated with large fire occurrence in Mediterranean France: evidence for a wind-driven fire regime. *International Journal of Climatology*, 37(1), 524–533.

Ruffault, J., StPaul, N.M., Pimont, F. and Dupuy, J.L. (2018a) How well do meteorological drought indices predict live fuel moisture content (LFMC)? An assessment for wildfire research and operations in Mediterranean ecosystems. *Agricultural and Forest Meteorology*, 262, 391–401.

Russo, A., Gouveia, C.M., Páscoa, P., da Câmara, C.C., Sousa, P.M. and Trigo, R.M. (2017) Assessing the role of drought events on wildfires in the Iberian Peninsula. *Agricultural and Forest Meteorology*, 237, 50–59.

Sánchez-Benítez, A., García-Herrera, R., Barriopedro, D., Sousa, P. M. and Trigo, R.M. (2018) June 2017: the earliest European summer mega-heatwave of reanalysis period. *Geophysical Research Letters*, 45(4), 1955–1962.

San-Miguel-Ayanz, J., Durrant, T., Boca, R., Liberta, G., Branco, A., Rigo, D., Ferrari, D., Maianti, P., Vivancos, T., Oom, D., Pfeiffer, H., Loffler, P., Nuijten, D., Leray, T. and Oom, D. (2019). Forest fires in Europe, Middle East and North Africa 2018. Joint Research Center, CE: EUR 29856. p. 178.

San-Miguel-Ayanz, J., Moreno, J.M. and Camia, A. (2013) Analysis of large fires in European Mediterranean landscapes: lessons learned and perspectives. *Forest Ecology and Management*, 294, 11–22.

Sharples, J.J. and McRae, R.H. (2011) Evaluation of a very simple model for predicting the moisture content of eucalypt litter. *International Journal of Wildland Fire*, 20(8), 1000–1005.

Silva, J.M., Moreno, M.V., LePage, Y., Oom, D., Bistinas, I. and Pereira, J.M.C. (2019) Spatiotemporal trends of area burned in the Iberian Peninsula, 1975–2013. *Regional Environmental Change*, 19(2), 515–527.

Silva JS, Rego FC, Fernandes P and Rigolot, E. (2010). *Towards integrated fire management: outcomes of the European project fire paradox*. European Forest Institute, Research Report 23. p. 244.

Simard, A.J. and Main, W.A. (1982) Comparing methods of predicting jack pine slash moisture. *Canadian Journal of Forest Research*, 12(4), 793–802.

Skinner, W.R., Flannigan, M.D., Stocks, B.J., Martell, D.L., Wotton, B.M., Todd, J.B., Mason, J.A., Logan, K.A. and Bosch, E.M. (2002) A 500 hPa synoptic wildland fire climatology for large Canadian forest fires, 1959–1996. *Theoretical and Applied Climatology*, 71(3–4), 157–169.

Soriano, L.R., Tomás, C., de Pablo, F. and García, E. (2013) Circulation weather types and wildland forest fires in the western Iberian Peninsula. *International Journal of Climatology*, 33(6), 1401–1408.

Swetnam, T.W. and Betancourt, J.L. (1998) Mesoscale disturbance and ecological response to decadal climatic variability in the American southwest. *Journal of Climate*, 11(12), 3128–3147.

Tedim, F., Leone, V., Amraoui, M., Bouillon, C., Coughlan, M.R., Delogu, G.M., Fernandes, P.M., Ferreira, C., McCaffrey, S., McGee, T.K., Parente, J., Paton, D., Pereira, M.G., Ribeiro, L. M., Viegas, D.X. and Xanthopoulos, G. (2018) Defining extreme wildfire events: difficulties, challenges, and impacts. *Fire*, 1(1), 9.

Tedim, F., Leone, V., Coughlan, M., Bouillon, C., Xanthopoulos, G., Royé, D., Correia, J.M.F. and Ferreira, C. (2020b) Extreme wildfire events: the definition. In: *Extreme Wildfire Events and Disasters, Root Causes and New Management Strategies*. Amsterdam: Elsevier, pp. 3–29.

Tedim, F., Leone, V., McCaffrey, S., McGee, T.K., Coughlan, M., Correia, F.J. and Magalhães, C.G. (2020a) Safety enhancement in extreme wildfire events. In: *Extreme Wildfire Events and Disasters, Root Causes and New Management Strategies*. Amsterdam: Elsevier, pp. 91–115.

Tramblay, Y., Koutroulis, A., Samaniego, L., Vicente-Serrano, S.M., Volaire, F., Boone, A., Le Page, M., Llasat, M.C., Albergel, C., Burak, S., Cailleret, M., Kalin, K.C., Davi, H., Dupuy, J.L., Greve, P., Grillakis, M., Hanich, L., Jarlan, L., Martin-StPaul, N., Martínez-Vilalta, J., Mouillot, F., Pulido-Velazquez, D., Quintana-Seguí, P., Renard, D., Turco, M., Türkeş, M., Trigo, R., Vidal, J.P., Vilagrosa, A., Zribi, M. and Polcher, J. (2020) Challenges for drought assessment in the Mediterranean region under future climate scenarios. *Earth-Science Reviews*, 210, 103348.

Trigo, R.M. and DaCâmara, C.C. (2000) Circulation weather types and their influence on the precipitation regime in Portugal. *International Journal of Climatology*, 20(13), 1559–1581.

Trigo, R.M., Pereira, J.M., Pereira, M.G., Mota, B., Calado, T.J., da Câmara, C.C. and Santo, F.E. (2006) Atmospheric conditions associated with the exceptional fire season of 2003 in Portugal. *International Journal of Climatology*, 26(13), 1741–1757.

Trigo, R.M., Sousa, P.M., Pereira, M.G., Rasilla, D. and Gouveia, C. M. (2016) Modelling wildfire activity in Iberia with different atmospheric circulation weather types. *International Journal of Climatology*, 36(7), 2761–2778.

Turco, M., Jerez, S., Augusto, S., Tarín-Carrasco, P., Ratola, N., Jiménez-Guerrero, P. and Trigo, R.M. (2019) Climate drivers of the 2017 devastating fires in Portugal. *Scientific Reports*, 9(1), 1–8.

Turco, M., von Hardenberg, J., AghaKouchak, A., Llasat, M.C., Provenzale, A. and Trigo, R.M. (2017) On the key role of droughts in the dynamics of summer fires in Mediterranean Europe. *Scientific Reports*, 7(1), 1–10.

Van Wagner, C.E. (1974) *Structure of the Canadian Forest Fire Weather Index*. Ottawa: Canadian Forestry Service Publications n. 1333.

Van Wagner, C.E. (1990) Six decades of forest fire science in Canada. *The Forestry Chronicle*, 66(2), 133–137.

Viegas, D.X., Almeida, M.F. and Ribeiro, L.M. (Eds.). (2017) *O complexo de incêndios de Pedrógão Grande e concelhos limítrofes, iniciado a 17 de junho de 2017. Centro de Estudos sobre Incêndios Florestais ADAI/LAETA*. Coimbra: Universidade de Coimbra.

Viegas, D.X., Almeida, M.F. and Ribeiro, L.M. (eds.). 2019. Análise dos Incêndios Florestais Ocorridos a 15 de outubro de 2017. Centro de Estudos sobre Incêndios Florestais ADAI/LAETA, Universidade de Coimbra, Coimbra.

Viegas, D.X., Soares, J. and Almeida, M. (2013) Combustibility of a mixture of live and dead fuel components. *International Journal of Wildland Fire*, 22(7), 992–1002.

Viegas, D.X. and Viegas, M.T. (1994) A relationship between rainfall and burned area for Portugal. *International Journal of Wildland Fire*, 4(1), 11–16.

Viegas, D.X., Viegas, M.T. and Ferreira, A.D. (1992) Moisture content of fine forest fuels and fire occurrence in Central Portugal. *International Journal of Wildland Fire*, 2(2), 69–86.

Westerling, A.L.R. (2016) Increasing western US forest wildfire activity: sensitivity to changes in the timing of spring. *Philosophical Transactions of the Royal Society B: Biological Sciences*, 371, 20150178.

Wotton, B.M. (2008) Interpreting and using outputs from the Canadian Forest Fire Danger Rating System in research applications. *Environmental and Ecological Statistics*, 16(2), 107–131.

SUPPORTING INFORMATION

Additional supporting information may be found in the online version of the article at the publisher's website.

How to cite this article: Carmo, M., Ferreira, J., Mendes, M., Silva, Á., Silva, P., Alves, D., Reis, L., Novo, I., & Xavier Viegas, D. (2021). The climatology of extreme wildfires in Portugal, 1980–2018: Contributions to forecasting and preparedness. *International Journal of Climatology*, 1–24. https://doi.org/10.1002/joc.7411

APPENDIX A.

TABLE A1 Summary table of characteristics, drought indices, and previous accumulated precipitation for each EWP

EWP dates and burned area				Drought indices			Preceding accumulated rainfall				
Start–end	Duration (days)	Mean daily burned area (ha)	Total burned area (ha)	DC	FFMC	PDSI	64 Days (mm)	32 Days (mm)	16 Days (mm)	8 Days (mm)	64-Days anomaly (mm)
26 July 1981–30 July 1981	5	4,036	20,180	316	94	−0.8	35.3	9.2	0.0	0.0	−18.4
22 September 1983–29 September 1983	8	3,496	27,971	361	92	−1.1	44.7	12.8	2.6	1.5	3.4
27 August 1985–30 August 1985	4	3,191	12,765	343	93	−0.2	19.4	4.8	1.3	0.5	−8.0
10 September 1985–17 September 1985	8	4,704	37,631	394	92	−2.1	10.1	3.8	2.5	2.4	−17.8
13 July 1986–21 July 1986	9	3,694	33,250	261	92	−1.9	19.8	14.1	0.1	0.1	−57.2
13 September 1987–19 September 1987	7	3,161	22,125	365	94	0.5	51.7	36.5	30.8	0.0	22.7
25 July 1989–2 August 1989	9	3,050	27,447	220	92	−1.4	100.6	10.7	7.1	7.0	45.2
10 July1990–13 July 1990	4	3,595	14,379	253	94	−2.5	29.7	9.2	3.0	0.3	−53.7
18 July 1990–21 July 1990	4	3,398	13,594	290	94	−2.5	18.2	6.0	0.7	0.4	−48.8
3 August 1990–12 August 1990	10	6,068	60,681	350	94	−2.1	20.8	8.6	7.9	4.5	−20.3
26 June 1991–30 June 1991	5	3,029	15,146	215	92	−3.0	28.3	23.7	0.3	0.3	−77.8
16 July 1991–20 July 1991	5	6,663	33,316	300	95	−2.7	27.4	3.8	3.6	0.1	−42.2
4 August 1991–18 August 1991	15	5,758	86,369	378	93	−2.3	24.0	9.1	5.7	3.1	−15.7
6 August 1992–10 August 1992	5	5,638	28,191	339	95	−0.4	44.7	5.8	3.7	3.4	7.2
23 July 1995–29 July 1995	7	3,939	27,570	327	94	−2.5	52.5	43.7	15.4	0.4	−5.7
10 August 1995–17 August 1995	8	4,964	39,713	398	91	−2.6	54.3	12.9	4.9	3.4	18.4
25 August 1995–31 August 1995	7	5,455	38,186	460	94	−2.6	49.4	5.7	0.8	0.4	21.6
29 August 1996–4 September 1996	7	3,272	22,907	385	91	−0.5	17.2	9.9	5.8	2.5	−11.0
1 August 1998–11 August 1998	11	4,682	51,503	244	91	−0.4	62.5	13.7	1.8	0.0	18.4
20 August 1998–26 August 1998	7	6,262	43,832	318	90	−0.4	19.0	6.8	5.0	4.5	−9.9
05 August 2000–12 August 2000	8	5,228	41,821	289	93	0.5	25.4	14.3	11.7	0.0	−13.1
16 August 2000–20 August 2000	5	3,337	16,684	334	93	0.5	22.5	12.5	0.7	0.6	−9.3
16 September 2001–19 September 2001	4	3,188	12,751	436	93	−0.5	29.0	13.6	0.7	0.0	−3.2
13 July 2002–19 July 2002	7	3,780	26,461	238	90	−1.6	45.5	11.2	5.7	4.8	−31.4
24 July 2002–31 July 2002	8	3,164	25,312	281	91	−1.6	37.6	12.8	8.1	3.3	−19.1
29 July 2003–18 August 2003	21	17,617	369,956	288	93	−2.5	40.5	29.0	13.7	1.7	−7.7
10 September 2003–19 September 2003	10	4,351	43,507	421	92	−2.5	38.6	22.3	18.9	2.5	10.6
29 June 2004–2 July 2004	4	3,209	12,836	189	94	−3.3	65.6	8.6	5.1	4.8	−34.9
14 July 2004–17 July 2004	4	3,325	13,298	249	94	−3.3	41.1	8.2	3.1	3.0	−33.7
24 July 2004–30 July 2004	7	9,993	69,950	294	95	−3.3	38.6	7.2	1.5	0.4	−18.1
8 July 2005–13 July 2005	6	3,220	19,322	346	93	−4.2	49.2	9.0	4.7	0.3	−38.6
19 July 2005–25 July 2005	7	4,752	33,262	395	93	−4.2	22.0	6.2	0.3	0.3	−43.6
3 August 2005–9 August 2005	7	9,384	65,685	449	94	−4.1	17.1	7.3	7.0	6.1	−24.0

(Continues)

TABLE A1 (Continued)

EWP dates and burned area				Drought indices			Preceding accumulated rainfall				
Start–end	Duration (days)	Mean daily burned area (ha)	Total burned area (ha)	DC	FFMC	PDSI	64 Days (mm)	32 Days (mm)	16 Days (mm)	8 Days (mm)	64-Days anomaly (mm)
13 August 2005–24 August 2005	12	10,648	127,777	481	93	−4.1	20.7	11.9	6.4	4.6	−12.7
2 October 2005–5 October 2005	4	3,139	12,556	612	93	−1.6	21.0	16.1	0.8	0.3	−36.9
4 August 2006–14 August 2006	11	3,839	42,229	321	93	−1.0	49.9	9.6	3.1	0.4	10.2
29 August 2009–3 September 2009	6	4,118	24,710	422	93	−2.2	29.9	4.5	1.2	0.2	1.7
25 July 2010–29 July 2010	5	3,307	16,536	242	95	0.2	49.2	9.0	0.7	0.2	−6.2
3 August 2010–19 August 2010	17	4,786	81,370	283	93	−1.0	41.9	3.1	0.3	0.1	0.7
27 August 2010–31 August 2010	5	3,163	15,813	382	91	−1.0	11.4	2.4	1.6	1.2	−16.0
18 July 2012–20 July 2012	3	10,252	30,756	311	95	−3.7	29.1	8.5	2.0	0.4	−37.8
1 September 2012–7 September 2012	7	4,330	30,308	462	94	−2.3	17.4	11.4	1.6	1.5	−11.0
19 August 2013–31 August 2013	13	6,003	78,040	416	93	−1.3	16.0	5.5	0.4	0.1	−13.8
6 August 2016–16 August 2016	11	9,528	104,810	299	94	0.9	22.1	8.3	0.4	0.4	−15.4
3 September 2016–9 September 2016	7	3,409	23,863	412	93	−0.5	13.1	4.2	3.4	0.9	−14.9
17 June 2017–24 June 2017	8	6,797	54,378	171	95	−3.2	79.6	12.7	1.6	0.4	−45.1
16 July 2017–21 July 2017	6	3,864	23,182	274	94	−3.1	32.5	17.2	7.4	0.5	−37.0
23 July 2017–27 July 2017	5	8,385	41,926	303	91	−3.1	29.9	15.9	3.1	0.8	−28.2
11 August 2017–16 August 2017	6	7,966	47,799	383	94	−2.9	19.1	1.6	0.7	0.1	−16.4
23 August 2017–29 August 2017	7	3,548	24,839	435	93	−2.9	16.7	0.9	0.1	0.0	−11.6
6 October 2017–10 October 2017	5	3,207	16,037	546	93	−4.1	12.6	1.4	0.6	0.1	−53.3
15 October 2017–17 October 2017	3	56,505	169,516	572	94	−4.1	12.6	0.9	0.1	0.0	−71.9
3 August 2018–10 August 2018	8	3,582	28,655	239	96	0.2	67.5	10.2	1.3	0.4	26.4

Note: DC, FFMC, and accumulated rainfall were obtained from ERA5 reanalysis grid estimates, averaged over Portugal from 165 points (DOI: 10.24381/cds.0e89c522), while PDSI was calculated from IPMA meteorological stations in Portugal (www.ipma.pt/en/oclima/observatorio.secas).